AD-A070 257 OPTICAL DESIGN SERVICE TUCSON AZ F/G 20/6
DEVELOPMENT OF TECHNIQUES FOR THE DESIGN OF ATHEMALIZED OPTICAL--ETC(U)
NOV 78 R A BUCHROEDER DAAK40-78-M-0077

UNCLASSIFIED NL

| OF |

AD
A070257

END
DATE
FILMED
8-79
DDC

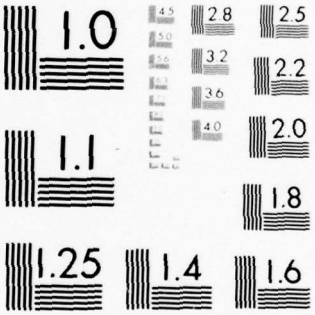

MICROCOPY RESOLUTION TEST CHART
NATIONAL BUREAU OF STANDARDS 1963 A

LEVEL II

2

AD A070257

Report ~~ODS-DAAK40~~-78-R-0085

DEVELOPMENT OF TECHNIQUES FOR THE
DESIGN OF ATHERMALIZED OPTICAL SYSTEMS

A theoretical study dealing with
boresight and focus stability and
compensation.

Dr. R. A. Buchroeder
OPTICAL DESIGN SERVICE
5436 N. Kennebec Lane
Tucson, Arizona 85704

1 November 1978

Final report for the Period 1 April 1978 - 1 November 1978

For Public Release
Distribution Unlimited

DDC FILE COPY

DDC
RECEIVED
JUN 22 1979
D

Prepared for

United States Army Missile
Research and Development Command
Redstone Arsenal, Alabama 35809

79 06 15 058

UNCLASSIFIED

SECURITY CLASSIFICATION OF THIS PAGE (When Data Entered)

REPORT DOCUMENTATION PAGE

READ INSTRUCTIONS BEFORE COMPLETING FORM

1. REPORT NUMBER: ODS-~~DAAK40-78-R-0085~~

2. GOVT ACCESSION NO.

3. RECIPIENT'S CATALOG NUMBER

4. TITLE (and Subtitle): (6) DEVELOPMENT OF TECHNIQUES FOR THE DESIGN OF ATHEMALIZED OPTICAL SYSTEMS,

5. TYPE OF REPORT & PERIOD COVERED: Technical Report

6. PERFORMING ORG. REPORT NUMBER: ~~ODS-DAAK40-78-R-0085~~

7. AUTHOR(s): (10) R. A. Buchroeder

8. CONTRACT OR GRANT NUMBER(s): (15) DAAK40-78-M-0077

9. PERFORMING ORGANIZATION NAME AND ADDRESS:
Optical Design Service
5436 N. Kennebec Lane
Tucson, Arizona 85704

10. PROGRAM ELEMENT, PROJECT, TASK AREA & WORK UNIT NUMBERS:
~~AMCMS #611102H49001~~
PRON #A187G034D8D3-01

11. CONTROLLING OFFICE NAME AND ADDRESS:
U. S. Army Missile R & D Command
DRDMI - TGP
Redstone Arsenal, Alabama 35809

12. REPORT DATE: (11) 1 Nov~~ember 19~~78

13. NUMBER OF PAGES: 58

14. MONITORING AGENCY NAME & ADDRESS (if different from Controlling Office): (9) Final rept. 1 Apr - 1 Nov 78,

15. SECURITY CLASS. (of this report): Unclassified

15a. DECLASSIFICATION/DOWNGRADING SCHEDULE

16. DISTRIBUTION STATEMENT (of this Report): (12) 66p.

For Public Release
Distribution Unlimited

17. DISTRIBUTION STATEMENT (of the abstract entered in Block 20, if different from Report)

18. SUPPLEMENTARY NOTES

19. KEY WORDS (Continue on reverse side if necessary and identify by block number)

Optics, Optical Design, Lens Design, Geometrical Optics, Athermalization

20. ABSTRACT (Continue on reverse side if necessary and identify by block number)

A theory and practice for athermalizing focus and boresight errors in optical systems is presented. Thermal properties of optical materials, mainly for the visible spectrum, are surveyed. Designs techniques are suggested.

DD FORM 1 JAN 73 1473 EDITION OF 1 NOV 65 IS OBSOLETE

UNCLASSIFIED

SECURITY CLASSIFICATION OF THIS PAGE (When Data Entered)

S/C 394 100

79 06 15 055

TABLE OF CONTENTS

Section		Page
	LIST OF ILLUSTRATIONS	i
	LIST OF TABLES	iv
1.	SUMMARY AND INTRODUCTION	
	1.1 Summary	1
	1.2 Introduction	1
2.	PERFORMANCE CONSIDERATIONS	4
	2.1 Defocus	4
	2.2 Central Obscuration	5
	2.3 Boresight Error	6
	2.4 Error Budget	6
	2.5 Merit Function	8
3.	WAVE ABERRATION THEORY	9
	3.1 First Order Generation and Propagation of Wavefronts	9
	3.2 Application of the OPD Method	12
	3.3 Snell's Law in Paraxial Form	13
	3.4 Defocus	14
	3.4.1 Thickness or Airspace Error	14
	3.4.2 Radius Error	14
	3.4.3 Refractive Index Error	15
	3.5 Boresight Error	15
	3.5.1 Decentered Optical Surface	15
	3.5.2 Tilted Optical Surface	16
	3.5.3 Image Tilt	16
	3.6 Diffraction Gratings	17
	3.7 Surface Power Athermalization	17
	3.8 Thickness Athermalization	18
	3.9 Linear Radial Gradient	18
	3.10 Linear Axial Gradient	19
	3.11 Linear Transverse Gradient	20
	3.12 Thin Prism (Wedge)	20
	3.13 Tilted Plane Surface	21
	3.14 Plane Parallel Glass Plate: Defocus	22
	3.15 Plane Parallel Glass Plate: Boresight	23
	3.16 Chromatic Aberration	24
	3.17 "Decentered" Spherical Aberration	24
	3.18 Raytrace Test of Theory	26

ccession For
TIS GRA&I
DC TAB
Unannounced
Justification
By
Distribution/
Availability Codes
Dist | Avail and/or special
A

TABLE OF CONTENTS--continued

Section		Page
4.	OPTICAL MATERIALS	29
	4.1 Discussion	29
	4.2 Dielectric Filters	29
	4.3 Optical Glass	30
	4.4 Plastics	35
	4.5 Fluids	36
	4.6 Mirror Substrates	37
	4.7 Mechanical Materials	38
5.	DESIGN TECHNIQUES	39
	5.1 Discussion	39
	5.2 Achromatic Lens	39
	5.3 Mirror Folds for Stability	43
	5.4 Optical Lever Compensation	44
	5.5 Inertial Reference	45
	5.6 Zoom Lens	49
6.	CONCLUSIONS AND RECOMMENDATIONS	53
	6.1 Conclusions	53
	6.2 Recommendations	53
	SELECTED BIBLIOGRAPHY	55

LIST OF ILLUSTRATIONS

Figure		Page
1	MTF in the presence of defocussing	4
2	Effect of random wavefront error on central intensity	4
3	Diffraction Sine Wave Response with central obstruction	5
4	Radial energy distribution for a diffraction-limited aperture with circular central obscurations	5
5	General error budget for passive Optical System	7
6	First order propagation of wavefront aberration	10
7	Division of a complex system into simple units	11
8	OPD method used to determine refraction through a prism	12
9	OPD method used to determine refraction through a lens	13
10	Snell's Law at a refracting surface	13
11	Defocus and related OPD	14
12	Boresight aberration	15
13	Uniform temperature change causes length to change	18
14	Derivation of the effect of a radial thermal gradient	19
15	Proper derivation of the effect of an axial thermal gradient	19
16	Transverse thermal gradient leads to prismatic effect	20

LIST OF ILLUSTRATIONS--continued

Figure		Page
17	OPD generated by a thin prism or wedge	21
18	OPD generated by a tilted plane surface	21
19	Defocussing caused by disk of glass	22
20	Boresight error caused by tilted disk of glass	23
21	Conceptual layout and surface numbering of design used to test OPD theory	26
22	Measured variation of a typical filter with temperature	29
23	Wavelength shift as a function of temperature	29
24	Representative page from the Schott Optical Glass Catalog showing general information available to the optical designer ...	30
25	Variation of refractive index thermal coefficient with variation of atmospheric pressure	31
26	Temperature effect on thermal conductivity	31
27	Change of the refractive index of BK7	32
28	Change of refractive index from compression and tension	32
29	Temperature coefficient of refractive index of some optical glasses	33
30	Relative and absolute temperature coefficients of refractive index as functions of temperature (BK7 glass)	33
31	Thermal expansion of CER-VIT compared with ordinary fused silica	37
32	Data for homogeneous temperature athermalization.	40
33	Data for radial gradient athermalization	40
34	Data for selecting achromatic glass pairs for athermal doublets	41

LIST OF ILLUSTRATIONS--continued

Figure		Page
35	Concept of focus-compensated television sensor	41
36	Technique for maintaining parallelism of boresight axes.	43
37	Boresight stabilization using the optical lever	44
38	Symmetrical nature of image stabilizer	45
39	Fluid-filled relay image stabilizer concept	46
40	Image motion compensation using fluid filled prisms	47
41	Prism equivalent using lenses for image stabilization	47
42	Image stabilization based on lens decentration	48
43	Parameters of the moving elements in a mechanically compensated zoom	50
44	Zoom Imaging Section at extreme and mean magnifications	51

LIST OF TABLES

Table		Page
1	Specification of optical design used to test OPD theory	27
2	Thermal properties of Schott Optical Glass	34
3	Selected plastic materials for optical lens elements	35
4	Selected fluids for optical applications	36
5	Properties of Selected mirror substrate materials	37
6	Thermal expansion of selected materials useable for mechanical elements	38
7	Representative zoom Separations relative to principal planes	50
8	OPD Tolerance analysis of group decentrations in sample design. (*derives from goal of .014mm image runout)	52

1. SUMMARY AND INTRODUCTION

1.1 SUMMARY

This report describes a theoretical investigation of optical materials and design techniques for achieving athermalized focus and boresight. Although dealing primarily with the visible spectrum, the results apply equally to any system whose behavior can be described with gaussian theory.

The investigation deals mainly with homogeneous thermal soak, to a lesser extent with simple thermal gradients, and not at all with the atmosphere and other effects external to the optics. Regretfully, it has only been possible to warn of the complexities of inhomogeneous refractive index accompanying thermal gradients, which result in peculiar and formidable problems in the analysis of prisms.

The wave aberration theoretical technique, already rapidly displacing geometrical techniques in the specification and analysis of optical components and images, is now applied to focus and boresight. It is suggested that this technique provides greater economy and insight than older techniques, and is a logical development toward establishing a homogeneous merit function for system performance. Following development of the wave theory as applied to focus and boresight, the accuracy of theory is demonstrated by exact raytracing.

It is explained that while certain optical systems can be athermalized in retrospect rather than during component optimization, better results are achieved by introducing thermal considerations at the outset of the design process. The designer has at his desposal a wide variety of special glass types, as well as a conventional array of plastics, fluids, high and low expansion mechanical materials, all of which can be included in the process of first-order layout to maximize resistance to thermally-induced deterioration of performance. The properties of selected materials are documented, and a number of techniques for athermalized design are illustrated.

1.2 INTRODUCTION

The majority of older techniques for tolerancing boresight and focus are based on the empirical approach of repeatedly raytracing an optical system as each optical parameter is disturbed, then reset to its nominal value. The total allowable error is partitioned according to RSS theory assuming scaler combination of the errors. Modern performance requirements have become so stringent that it is unlikely the vector nature of errors can any longer be ignored, for the tolerances required to achieve absolute stability are inconsistent with light weight and portability.

We propose a comparatively new theory, based on the geometrical wave theory of optics, which permits a vectorial interpretation of boresight and focus errors, and which provides greater economy of calculation coupled with strong perceptual insight. The wave theory has the further advantage that it is consistent with modern techniques of image analysis, so that should a system merit function be devised which must include focus and boresight, our theory is directly applicable.

Relative to global coordinate system, the effects of any kind of misalignment, vibration, thermal distortion, or element parameter error can be expressed as a wave aberration. Customarily, opticists deal with terms of the fourth order to describe failure of the system to produce a stigmatic image; the second order terms, which pertain to focus and boresight,have been given little attention. However, nearly all prior treatments deal with the rotationally symmetric optical system. Our purpose is to consider additionally the asymmetry resulting from thermal influence.

Theoretical consideration indicates that all simple errors can be dealt with using algebraic techniques. Peculiar effects, such as stress-induced birefringence and nonlinear distortions are beyond the scope of the present investigation.

This report is limited in its scope to basic theory; however, exact raytracing has been performed to test agreement with low order calculations. No exceptions have been found to the qualitative prediction of boresight and focus error, and indeed quantitative agreement has been found exceptionally good.

We are concerned only with the basic optical system. We disregard atmospheric and airflow effects. Our emphasis is on homogeneous temperature distribution, but we discuss thermal gradients to the extent our understanding of the subject permits.

A great advantage of the wave method of analysis is that the cause of boresight and focus error has a physical meaning, clear by inspection, and requires no calculation to be understood. To quantify the effects, we have shown how to calculate the sign and magnitude of wave aberration arising from any homogeneous thermal disturbance of windows, lenses, mirrors and prisms. We use the convention of analytic geometry, however other conventions are known and the reader is free to chose his own.

The principles of athermal design divide into two classes. The first deals with preventing the separate components from changing focus and boresight. The athermalized achromatic lens is an example. The second class deals with flexible elements, using cross-correction to achieve stabilization. The two techniques can be used together for maximum compensation of thermal distortion. We suggest that when an inertial reference, such as gravity, is available, great accuracy can be obtained by coupling the optical system to it.

A great variety of optical materials is available. The properties of optical glass, plastic, liquids, mirror materials, and ordinary cell

materials are sampled in several tables which we have compiled using manufacturers' catalogs and published data. No guarantee is made that our transcription is perfectly accurate, nor should one show absolute confidence in a manufacturer's data. We know of one case where a well-regarded plastics manufacturer has consistently listed the wrong sign for a critical thermal property.

We have provided conceptual layout and discussion of selected techniques for athermalizing optical systems. Originally we had intended to deal with shared aperture and parallel aperture optical systems, however we realized the tolerancing of a pair of optical trains to each other was sensibly indentical to tolerancing any one system to a global coordinate system. We had also intended an ambitious discussion of zoom systems, but came to realize this could constitute a report in itself. A more modest discussion resulted.

A Selected Bibliography is provided which may of some value to the reader who wishes to study various facets of the topic in greater detail.

2. PERFORMANCE CONSIDERATIONS

2.1 DEFOCUS

Modulation transfer function (MTF) and encircled energy are two key indicators of the quality of focus. Assuming an otherwise perfect optical system, the effects of defocus are indicated in Figs. 1 and 2.

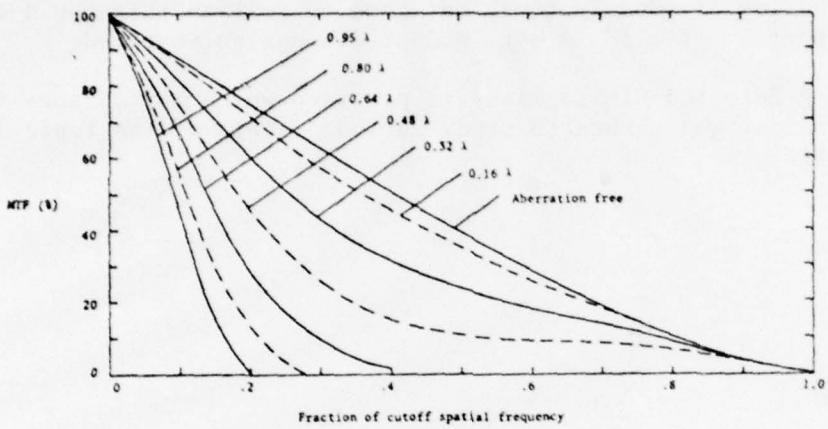

Fig. 1. MTF in the presence of defocussing.

Defocussing produces a symmetrical point spread function, a saving grace for boresight. However, the uncertainty with which the centroid can be found is reduced for stellar targets, and becomes confused if the target is buried in background clutter competing for recognition.

Error budgets usually deal with RMS values. The RMS value of defocus equals the peak-to-valley (P-V) defocus divided by 3.46.

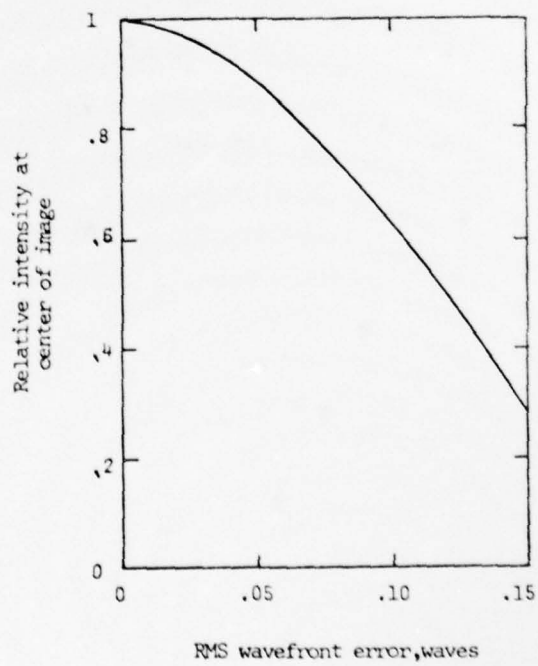

Fig. 2. Effect of random wavefront error on central intensity.

2.2 CENTRAL OBSCURATION

The existance of a central obscuration, typical in reflective systems, causes light to be spread out from the central Airy disc into the outer diffraction rings. This causes the effects on MTF and encircled energy shown in Figs. 3 and 4. In deciding whether to use a refractor or reflector, the matter of central obscuration often decides the matter. All things being equal, it would seem that the refractor might have a more liberal error budget because it has a higher nominal MTF and smaller radius of given encircled energy than its reflective counterpart. In recent years, however, we have seen a rapid development of unobscured, off-axis reflectors.

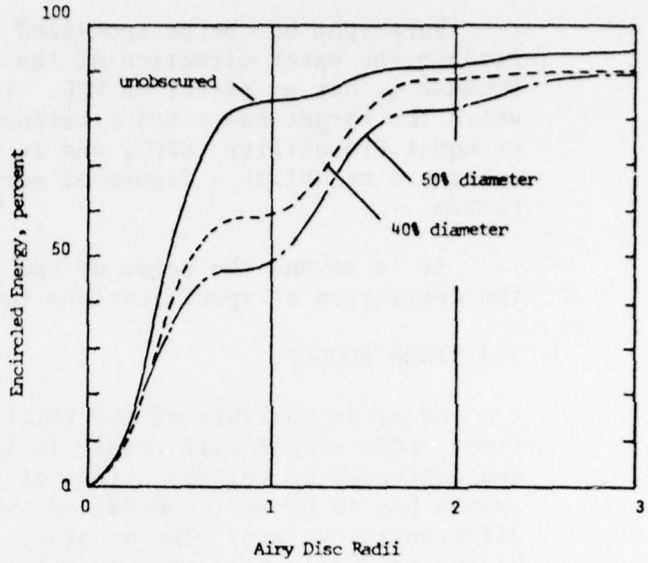

Fig. 4. Radial energy distribution for a diffraction-limited aperture with circular central obscurations.

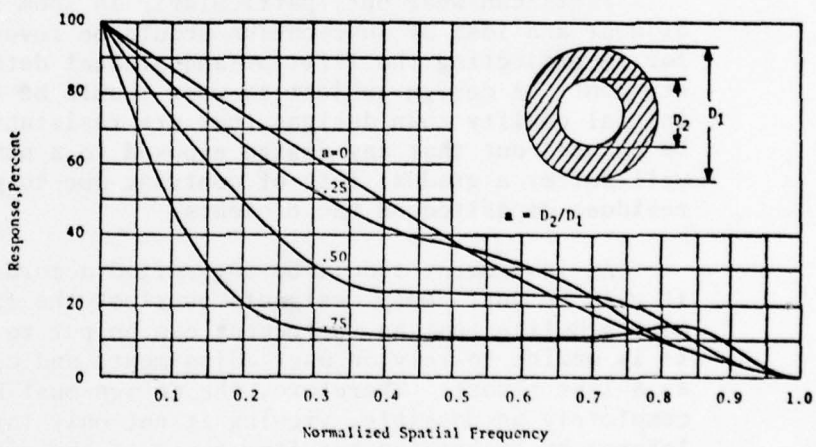

Fig. 3. Diffraction Sine Wave Response with central obstruction.

2.3 BORESIGHT ERROR

Boresight has be be specified in terms of a probability function, because the exact direction of the axis is never perfectly known, and because it has no effect on MTF. The diameter of a circle within which the target has a 50% likelihood of falling is known as the Circle of Equal Probability (CEP), and is used along with MTF or encircled energy to establish a figure of merit for a pointing or tracking system.

It is beyond the scope of the present investigation to deal with the derivation of specifications for CEP.

2.4 ERROR BUDGET

An error analysis of the total system has to be performed. The first order errors will result in inaccurate determination of angle and distance, as well as a loss of contrast (MTF). The nature of the system has to be well understood: whether it is to measure absolute or differential values. The accuracy required to acquire a target may be coarse, while precision is required for centering and discrimination of detail.

When a large system is moved, it requires some settling time before precise measurements can be taken, This reflects on the mechanical design of the instrument, however the optical layout can readily affect the obtainable performance. It is also known that if an optical system is suddenly uncovered, it may require a long time to 'settle out'. The purpose of this report is to deal with athermalization which hopefully will also minimize the time required to reach an acceptable error level.

Parts can wear out, particularly in zoom systems. The effects of wear and loss of lubrication should be investigated and allowed for in projecting the lifetime and gradual deterioration of the instrument. A design subject to wear should be toleranced for greater initial quality than designs that are resistant to change. It should be pointed out that any design exposed to a non-laboratory evironment will suffer a gradual loss of contrast due to pitting of windows and residues deposited on the elements.

An instrument should be ruggedized according to the use to which it will be put. Many designers overlook the fact that possibly the most grueling test an instrument can be put to will occur in shipping. It is unwise to rely on user adjustments and calibration schemes except as a last resort. Therefore, the design must be thought through as completely as possible, viewing it not only through the eyes of a laboratory technician but from those of the eventual user.

We will deal mainly with the problem of tolerancing components for fabrication, assembly and alignment. The instrument will probably require some factory adjustment to reach specifications. That this is so can be understood by noting that modern precision pointing and tracking systems achieve better than microarcsecond accuracy. A tolerance analysis shows that components cannot be built to allow drop-in achievement of such quality. Therefore, the error analysis takes note of

this. Those defects of optical radius, thickness, tilt, centration, spacing and refractive index that can be eliminated by practical adjustment are removed from the error budget. The remaining defects are known as non-compensatable errors.

The non-compensatable errors of a system must combine to be within system tolerance. An example of a budget is illustrated in Fig. 5. In an uncompensated thermal system, the errors are mainly systematic rather than random, so that while not compensatable, they are surely repeatable. This kind of budget is different than the one which has been thermally compensated. It is reasonable to expect a good degree of randomness and the application of RSS tolerancing is reasonably valid.

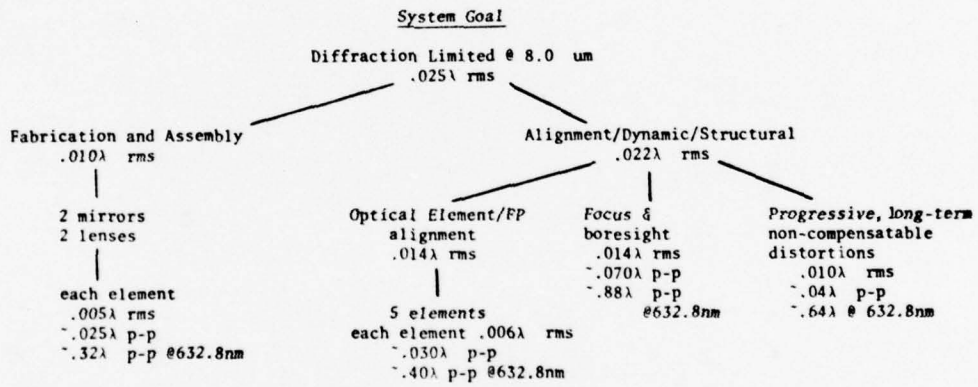

NOTE: Image jitter not included in this budget.

Fig. 5. General error budget for passive Optical System

2.5 MERIT FUNCTION

The merit functions used in lens optimization are based on some measure of transverse aberration, such as the RMS spot size, or on the wavefront variance. Defocus is included directly with the other aberrations in determining the plane of best focus. It is therefore natural to include defocus into a merit function for an athermalized lens. The use of a zoom program is ideal for optimization of performance, on the assumption sufficient experience has been gained to be sure the techniques work as well in practice as on paper.

Including boresight into the merit function is a bit more complicated, and involves some definition of the CEP. Since defocus and other imaging aberrations have a bearing on the CEP, along with boresight accuracy, weighting factors can be derived. The wave aberration form for boresight and defocus are logically computed along with the other image aberrations, so that a single figure of merit would seem possible.

3. WAVE ABERRATION THEORY

3.1 FIRST ORDER GENERATION AND PROPAGATION OF WAVEFRONTS

The wave theory of light, invented by Huygens and brought to a state of refinement for the optical designer by H. H. Hopkins, holds that each point on a luminous surface emits spherically expanding bundles of light, parts of which may be intercepted and utilized by an optical instrument. A surface of equal phase in the light bundle is termed a wavefront. The focussed point is actually blurred since not all the light emitted by the source is intercepted by the instrument, resulting in diffraction-limited reconstruction of the point image. The total image of the source equals this point spread function convolved with the geometrical image of the source.

Any departure from sphericity in the focussed wavefront results in a broadening of the point spread function, thus departures from a spherical reference sphere are considered aberrations. Some defects do not disturb the size of the point image, but affect its desired location relative to other points in the image. This is termed distortion. In practice, any departure from the desired focal point, either axially or laterally, may be treated as an aberration. Focus and boresight errors may be called aberrations since we so chose to define them.

A primary advantage of the wave theory is its simplicity. A technical advantage is that methods for computating diffraction-based imagery utilize wave theory in one fashion or other. The modulation transfer function, for example, is determined either from the convolution of the pupil function with itself, known as an autocorrelation, or from the Fourier transform of the diffraction-based point spread function, which itself is the Fourier transform of the pupil function. The pupil function is nothing more than wavefront departure from a sphere in the exit pupil.

An exact analysis of wave aberration is exceedingly complicated, but for our purpose wave theory is simpler than geometrical raytracing. We shall deal only with first approximations, and these we shall find extremely straightforward. We believe the designer using wave theory will become more comfortable in tolerancing focus and boresight errors than he was with alternate models of the problem.

At the first order level, also termed second order wave theory, we will deal only with algebraic calculations. All curves, spherical or aspheric, behave like parabolas. Cosines become unity, sines and tangents become *equal*. We deal with infinitesimal quantities in our derivations, yet the results are highly useful for very significant disturbances to the normal design. At this level, only focus, phase and boresight errors exist. Chromatic aberrations are simply the change of these with wavelength. Errors arise from disturbances to the nominal construction of the system: changes in curvature, spacing, refractive index, dispersion, and centration.

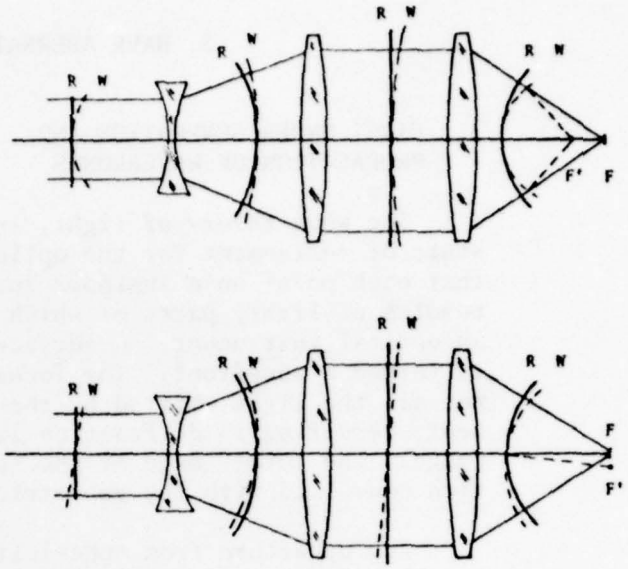

Fig. 6. First order propagation of wavefront aberration.

The nice thing about low order aberrations (up to the third order in transverse terms, or correspondingly the fourth order in wave aberration) is that they act separately from each other. One does not induce another, and we may add them up (vectorially if that be the case) *indefinitely*. The result is an output wavefront which has the sum of the defects contributed by each error source.

Fig. 6. attempts to illustrate the concept that the '*aberration*', wherever or however generated, propagates through the optical system and has, to the first approximation, the same magnitude and sign as when it was generated. There are no magnification factors or inversions involved, as is the case with raytracing methods. It is clear by inspection what the magnitude of the aberration is at all times. As we shall see, it is easy to calculate wave aberrations given only a single paraxial raytrace of the nominal optical design and a statement of the disturbances to each component.

Despite the advantages of computers, it is still good advice to keep things simple. An approach to this in optical analysis is to divide a complicated problem into fundamental parts as indicated in Fig. 7. All optical systems, at the first order level, and we include diffractive elements too, can be subdivided into just three fundamental optical units: the thin lens, the thin prism (wedge), and the plane-parallel disk of glass! It isn't asking much to remember the aberrations generated by these three simple units, but it would be overly demanding to tackle a complex optical system that had not been previously subdivided. Furthermore, without the benefit of simplification, valuable insights would be lost. Of course, as one gains experience with the wave theory, he develops his own building blocks for analysis. We merely wish to point out that tolerancing focus and boresight need not be an excruciating experience.

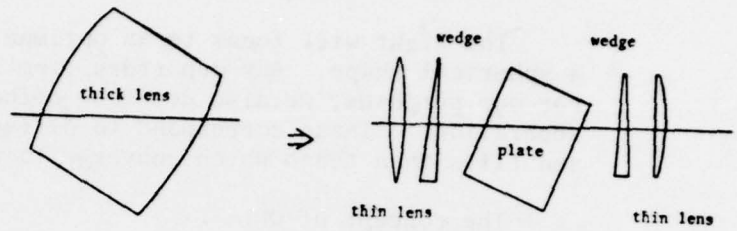

Fig. 7. Division of a complex system into simple units.

3.2 APPLICATION OF THE OPD METHOD

A wavefront is a mathematical abstraction, a surface of light all sections of which have spent an identical amount of time traveling from a single point source. The product of path length and refractive index along each path section is called the Optical Path Length, OPL.

The light will focus to an optimum point if the wavefront has a spherical shape. Any departure from sphericity is termed aberration. For our purposes, we also describe defocus and boresight error as aberrations. These correspond to different spherical wavefront shapes and tilts than those which converge to the desired image point.

The concept of OPL can be used to easily calculate the refraction, reflection, and diffraction of light. In this report, we will not concern ourselves with diffraction, that being too complex a field for our present interest.

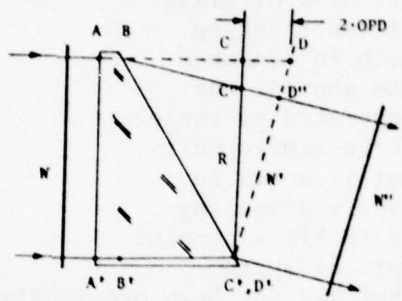

Fig. 8. OPD method used to determine refraction through a prism.

Consider Fig. 8, in which a prism refracts a beam of light. Light travels more *slowly in* glass than it does in air, and refractive index is the ratio of the speed of light in a vacuum to its speed in another medium like glass. The wavefront leaving the prism is a surface which has identical OPLs measured from the incident wavefront. OPL along A'B'C'D' equals that along ABC"D". However, first order theory sets cosines equal to unity, so that we can set ABC"D" equal to ABCD, a straight line. Similarly for any other incident line. Subracting BC from BD gives twice the OPD, since by convention we reference OPD to the axis. Since the prism tapers linearly, the output waveform must remain plane.

As shown in Fig. 9, we can apply the same thinking to refraction through a lens. The lens, however, has a curved shape rather than a simple taper. To the first approximation, any continuous curve with rotational symmetry can be expressed as a paraboloid. Therefore, the thickness of the lens decreases with the square of the distance off-axis, and OPD will thus increase quadratically with distance off axis. This is identical to saying the lens has power. The point which the output wave converges is its focal point, assuming the incident wave was flat. Otherwise, that image point is referred to as being conjugate to the object point. The same argument is applied to determine the focussing properties of a curved mirror.

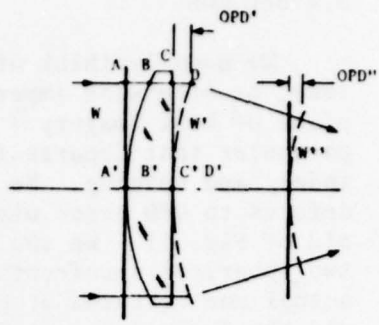

Fig. 9. OPD method used to determine refraction through a lens.

3.3 SNELL'S LAW IN PARAXIAL FORM

OPD theory is easily used to prove Snell's Law, N sinI = N'sinI'. We set the sines equal to the angles to obtain the paraxial form.

$$ni = n'i'$$

The geometry required for paraxial (first order) raytracing is shown in Fig. 10. If u is the incoming slope angle relative to the axis, i the angle of incidence (relative to the surface normal at the point of ray intersection), i' the angle of refraction (relative to the surface normal), d the separation to the next surface, and so forth, useable paraxial raytracing equations are given below.

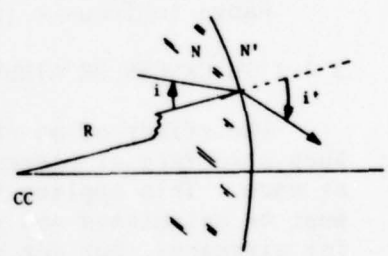

Fig. 10. Snell's Law at a refracting surface.

$$u = \text{incident slope}$$
$$i = y/R$$
$$i' = ni/n'$$
$$u' = u + i' - i$$
$$y' = u'd, \text{ repeat from "i"}$$

3.4 DEFOCUS

We usually think of defocus in terms of failing to focus the lens, or otherwise imperfectly making the detector line up with the plane of best imagery. Defocus also arises from any symmetrical parameter that departs from nominal: radius, thickness, refractive index, and spacing. We relate defocus to OPD error with the aid of Fig. 11. We see we have two spherical wavefronts, the actual one centered at F', and the desired one at F. The difference in radii is equal to the defocus. Using parabolic approximation, we can show that defocus and OPD are related by the expression,

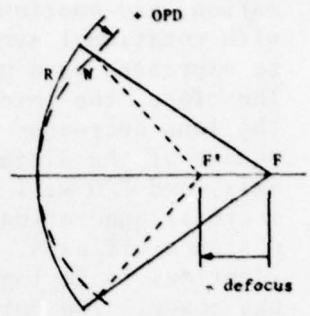

Fig. 11. Defocus and related OPD.

$$OPD = \frac{-\,y^2(\text{defocus})}{2R^2}$$

but y/R = -u', the numerical aperture, so

$$OPD = \frac{-(u')^2(\text{defocus})}{2} = \frac{-\,(\text{defocus})}{8\,(\,f/\#\,)^2}$$

In nominally collimated space, the error of a transmitter is readily determined from the OPD and the radius of the exit pupil.

Angular defocus = 2·OPD/(pupil radius)
Range to focus = (pupil radius^2/(2·OPD)

3.4.1 THICKNESS OR AIRSPACE ERROR

The effect of an error is to change local object distances. When a surface or element is moved, two spaces are usually changed at once. This applies to mirrors as well as lenses, and the results must be calculated and summed. We apply the defocus equation directly for airspaces, but for glass thickness errors, we multiply the glass thickness by (N-1)/N to obtain the air equivalent defocus.

3.4.2 RADIUS ERROR

An error in curvature adds or deletes "glass" at the margin of the ray bundle, which times the refractive index change at the surface equals OPD. For a single lens surface or mirror,

$$OPD + \frac{y^2}{2}(\,N' - N\,).(\,c' - c)$$

where c = 1/ radius of curvature

3.4.3 REFRACTIVE INDEX ERROR

A simple defocus occurs due to a change in the central airspace-equivalent as well as a change in surface refractive power. The former term is $\Delta N \cdot t / N^2$, which is then entered into the defocus equation.

Surface power can be written, $OPD = y^2(N'-N)/2R$, error in refractive index causes a defocus,

$$OPD = y^2 \cdot \Delta(N' - N)/2R$$

3.5 BORESIGHT ERROR

As shown in Fig. 12, boresight error relates to the lateral displacement of an image point. In collimated space, it is expressed as an angular error, and for a telescope objective or collimator, the angular boresight error is equal to the image displacement divided by the focal length.

Boresight errors are caused by unsymmetrical disturbances to the nominal system. However, if the optical path is folded with mirrors or prisms, the system is geometrically unsymmetrical and susceptable to boresight error even with isotropic temperature change.

A sign convention is indicated in the figure. The value of OPD is the beam radius multiplied by the tilt of the wavefront. Conversely, the angular boresight error is the OPD divided by the entrance pupil radius.

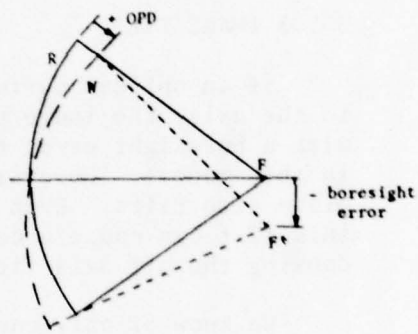

Fig. 12. Boresight aberration

3.5.1 DECENTERED OPTICAL SURFACE

If a surface is decentered by d, the wavefront will emerge tilted by $-(N' - N) \cdot d/R$, so that boresight OPD is,

$$OPD = \frac{-(N' - N) \cdot d \cdot y}{R}$$

For a curved mirror, the error equals $- d \cdot y/f$. For a lens the same result applies, as may be shown by adding up the effects of the two sides. For pure decentration, the thickness of the lens will not affect the predicted boresight error.

3.5.2 TILTED OPTICAL SURFACE

An individual optical surface, tilted about its vertex (the point of intersection of the surface with the axis) will have the same effect as a tilted plane surface. The angular deflection of the axis can be derived with Snell's Law. For a mirror, the OPD is instantly determined by knowing the angle of tilt and the radius of the axial beam.

For a thin lens, no deviation of the axis occurs because the principal points of the thin lens coincide with the center. The two sides thus cancel out each other's deflection. This is one of the advantages of breaking down a complex lens into thin lenses, wedges, and parallel glass slabs.

It is perhaps worth mentioning the reason a mirror doesn't act like a thin lens in this regard is that its principal points coincide not with the vertex, but with the center of curvature. To first order, a tilted mirror is equivalent to a decentered mirror. At the first order level, all mirrors are regarded as being parabolic so that whether the mirror is spherical or aspheric has no bearing on this observation.

3.5.3 IMAGE TILT

If an optical surface or element is decentered perpendicular to the axis, the image plane remains parallel to the object plane, with a boresight error that can be calculated by techniques described in this report. However, if a surface or element is tilted, the image plane also tilts. Even if it has no effect on focus or boresight, this tilt can cause a deterioration of instrument performance by causing the off-axis field to defocus.

We know of only one clearcut treatment of first order image tilt (Buchroeder, 1976) and present the general result without proof. We consider the case of a system with a finite focal point; for telescopic systems, the eyepiece can be separated from the objective, and angular divergence subsequently calculated.

$$\theta'_k = \frac{u_1}{u'_k}\,\theta_1 \quad - \frac{1}{u'_k} \quad \sum y_j\,\phi_j\beta_j$$

where u_1 and u'_k are the entrance and exit numerical apertures,

ϕ is the surface or element power, β is the tilt of the surface or element; and θ_1 and θ'_k are the tilts of the object and image planes

respectively. Note that if the input light is collimated, a tilt of the object has no effect on image tilt. A practical application of this equation is the Scheimpflug Effect, in which, for a single thin lens, the extensions of the lens diameter, the object plane, and the image plane must all intersect in a common line. The advantage of the formula is apparent for more complicated combinations of tilted and decentered elements.

While a tilted focal plane is of little significance in many instruments, it is likely to be of surprising concern in image stabilization devices.

3.6 DIFFRACTION GRATINGS

Holographic and conventionally produced gratings find use in an increasing number of modern optical systems, particularly those using lasers. Gratings can be used as beamsplitters or act directly in the imaging process. Their effectiveness is affected by thermal distortions.

It is beyond the scope of this investigation to consider holographic optical elements. Suffice it to say the change in quality of the element is directly related to the errors introduced into the fringe or ruling spacings. This effect is easily calculated for a plane grating used in collimated light. For normal incidence, the equation for a linear grating is,

$$n \cdot \lambda = d \sin \theta$$

differentiation and rearranging terms shows that the angular error is,

$$d = \frac{n \cdot \lambda \cdot \sec \theta \cdot \alpha \cdot \Delta T}{d}$$

As an example, a 20 line/mm grating on aluminum with 10 micrometer radiation will experience a 1 arc-second error for approximately each degree centrigrade of temperature change. One solution to this problem depends on maintaining fringe spacing despite temperature change. This poses problems, especially for high power laser applications where aluminum and copper mirrors are necessary.

3.7 SURFACE POWER ATHERMALIZATION

For the single reflecting surface case, only a zero expansion material provides freedom from defocus when temperature changes. For a lens, the refractive index change can offset the change in surface curvature. Most optical galsses have a tendency to be self-balancing, and many are very close to being self-cancelling at one wavelength.

The requirement for stablity is obtained by differentiating the expression for surface power.

$$\text{power} = \phi = \frac{N-N'}{R}, \text{ usually } \frac{N-1}{R}$$

$$\frac{d\phi}{dT} = 0 = R\,\frac{dN}{dT} - (n-1)\,\frac{dR}{dT}$$

$$\nu = \frac{\frac{dN}{dT}}{N-1} - \alpha$$

This is termed the thermal nu value of the glass, and if zero, the surface power is self-stabilized. Many optical glasses have negative as well as positive nus, so it is easy to design complex lenses athermalized for focus provided the temperature is homogeneous.

3.8 THICKNESS ATHERMALIZATION

No lens is perfectly thin, therefore its thickness change has an effect. With the aid of Fig. 13 it can be shown the condition to athermalize thickness effects on focus and phase is:

$$0 = \frac{\frac{dN}{dT}}{N-1} + \alpha$$

Therefore, when the effects of surface power are minimized, the effects of thickness are enhanced. In general, the effects of surface power are much more important.

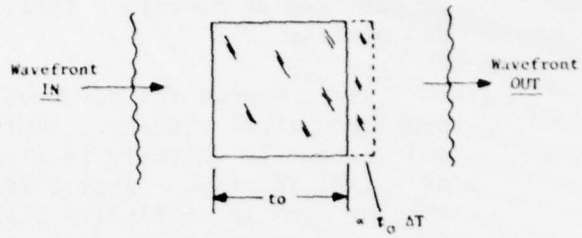

Fig. 13. Uniform temperature change causes length to change.

3.9 LINEAR RADIAL GRADIENT

Analysis of thermal gradients is virtually impossible unless we treat the optical element as being mechanically unrestrained. In practice, this is a reasonable approximation. Optical workers know that excessive tightening of lens retainers can easily cause astigmatism in the image. We are aware of no deliberate situation in which a designer has called out a 'press fit' on a lens to cell clearance, and for large lenses, it is customary to have a springy side restraint to allow for expansion and contraction of the lens cell. For large mirrors, elaborate floatation systems are constructed, eliminating, insofar as possible, friction and other restraint on the mirror.

Small elements such as prisms are held down with metal clamps; this occurs most commonly on low-resolution systems such as binoculars. The technique could be questionable for precision optics. Another practice that requires deliberation is the potting of elements. If the compound, usually RTV Silicone Rubber, is sufficiently compliant, little harm results if the potting is used for lateral restraint. Bonding to flat plates is more difficult and relies on the rigidity of the optical element to avoid distortion. The sensitivity of bonding stress can be appreciated by considering cemented doublet lenses only an inch or less in diameter. It has been found that if the mating curves mismatch in depth by more than 0.0001-inch, the shrinkage of a .001-inch cement layer can cause such warpage as to be visible in the transmitted image. It is good practice to match cemented faces to within two wavelengths of light.

Another approximation that proves reasonably accurate is treating lenses and mirrors as though they were plane parallel disks. This is fortunate, as arguments necessary to exactly deal with curves involve elaborate mathematics and the solutions are best handled with numerical methods.

Given these approximations, we are ready to consider how a disk will distort under a radial gradient, which for the moment we will assume linear from center to edge. Consider Fig. 14. The first opinion we could venture is that since the gradient is linear, perhaps the disk simply tapers uniformly from center to edge. But this is physically impossible, for there cannot be a discontinuity, or kink, at the center. We took a linear gradient to show the danger of intuitive thinking. The actual answer, regardless of whether the gradient is linear or not, is that the curvature on the faces must be given by a power series of even powered terms, the first term being derived by simple analysis.

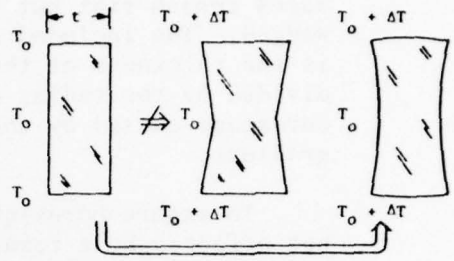

Fig. 14. Derivation of the effect of a radial thermal gradient.

$$\text{Deformation} = \frac{t}{2} \alpha \Delta T \rho^2$$

$$\text{OPD} = (N'-N) \frac{t}{2} \alpha \Delta T \rho^2$$

For a lens surface, the OPD is approximately

$$\frac{t}{4} \alpha \Delta T \rho^2$$

while for a mirror surface, it is

$$t \alpha \Delta T \rho^2.$$

3.10 LINEAR AXIAL GRADIENT

The same kind of reasoning is applied to an axial gradient, shown in Fig. 15. The disk becomes a meniscus lens, the derivation being as follows.

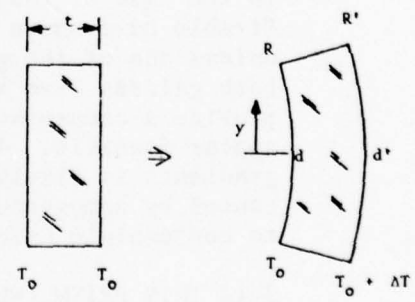

Fig. 15. Proper derivation of the effect of an axial thermal gradient.

$$d' - d = d\alpha \Delta T$$

$$R' = R + t$$

$$\frac{d}{R} = \frac{d'}{R'}$$

$$R = \frac{t}{\alpha \Delta T}$$

and $\text{OPD} = (N'-N) \frac{y^2}{2R}$ per surface.

For a mirror, $\text{OPD} = \frac{y^2 \alpha \Delta T}{t}$

3.11 LINEAR TRANSVERSE GRADIENT

Fig. 16 indicates this case is the linear axial gradient turned sideways. The optical faces remain flat but become wedged. The included angle is the thickness of the disk divided by the radius of curvature caused by the gradient.

To assure boresight is not affected by a transverse gradient, it is necessary for the refractive index of the glass to decrease if the material expands with an increase in temperature. This is unusual for optical glass, but typical of plastic, suggesting an unexplored advantage to plastic.

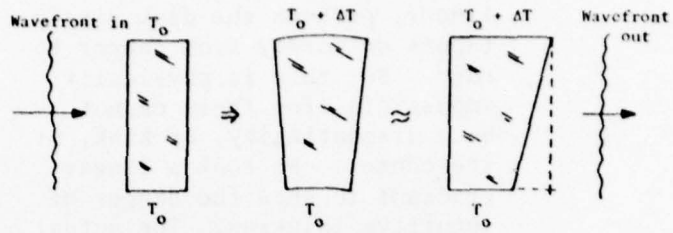

Fig. 16. Transverse thermal gradient leads to prismatic effect.

OPD theory can be applied to formalize the relationship insuring boresight accuracy in the presence of a transverse gradient. The same result applies to radial thermal gradients.

$$t_o\ (N_o + 1 \cdot \alpha \cdot \Delta T) = t_o\ (1 + \alpha \cdot \Delta T)(N_o + \frac{dN}{dT} \cdot \Delta T)$$

$$\frac{\frac{dN}{dT}}{N-1} + \alpha = 0$$

The expression to the left of the 'equals' sign is designated by the greek letter Gamma, and is positive for nearly all optical glass. In the case of lenses athermalized for radial gradients, Kohler and Strahle have shown it is impossible to achieve the desired result unless one of the glasses has a negative value for gamma, or unless both galsses have a zero value. The possibility of using plastic to provide a compensating material has not been investigated but would appear feasible. It is apparent that compensating a lens for radial gradients is likely to insure great sensitivity to simple defocus caused by homogenous thermal changes. Consequently, it is necessary to contemplate using special cell design to offset this latter effect.

3.12 THIN PRISM (WEDGE)

The analysis of prisms is simplified by separating them into thin fictious wedges plus an encapsulated plane parallel plate of glass. The plate is termed an orthoscopic unit magnification telescopic device, while the thin prisms are affine telescopic devices. When exact rays enter and leave the prism symmetrically, we have a condition termed minimum deviation, and the anamorphic magnification of the two prismatic segments is self cancelling.

To the first approximation, the tilt of a prism has no effect on boresight error, so we may set up the prism as shown in Fig. 17, which permits us to easily calculate the OPD of a thin prism. The same result can be obtained by doubly applying the paraxial form of Snell's Law for any other tilt of the thin prism.

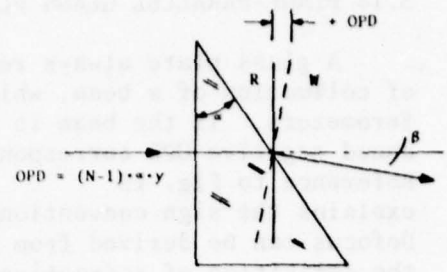

Fig. 17. OPD generated by a thin prism or wedge.

$$OPD = (N-1)\cdot\alpha\cdot y$$

The aberrated wavefront is taken to remain centered on the extension of the original ingoing axis by our freedom to select the reference sphere. Note that if we were analyzing an unsymmetrical optical system, our reference sphere might in fact be perpendicular to the outgoing, refracted ray. Relative to this axis, the aberrated wavefront would no longer be considered aberrated. An additional point is that the first order effects of disturbing the elements of an unsymmetrical optical system, such as a tilted component telescope, are virtually the same as obtained by eliminating the tilts and decentrations of the parent layout and analyzing it as a centered optical system, so unsymmetrical systems can be toleraced for boresight and focus using very simple techniques.

3.13 TILTED PLANE SURFACE

A tilted plane surface generates boresight error, but to the first approximation no change in focus. As suggested in Fig. 18, we interpret the aberrated wavefront as remaining centered on the extension of the ingoing axis rather than on the refracted axis. This applies to reflective surfaces as well. In actuality, the wavefront is centered on the refracted axis, but since it is just as permissable to decenter a reference sphere as it is to shift it axially, there is no first order consequence except to incompletely fill our presumed system exit pupil. This does not affect first order calculation of boresight error.

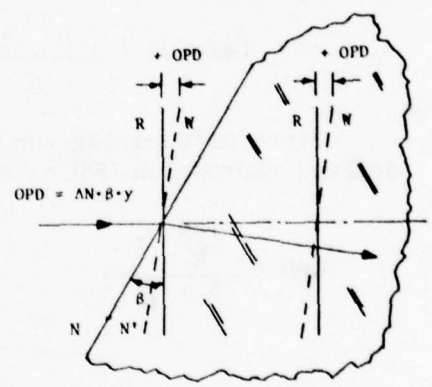

Fig. 18. OPD generated by a tilted plane surface.

The equation for OPD generated by a tilted plane surface is almost obvious by inspection,

$$OPD = \Delta N\cdot\beta\cdot y$$

so for a reflective surface, $OPD = 2\cdot\beta\cdot y$

3.14 PLANE-PARALLEL GLASS PLATE: DEFOCUS

A glass plate always retards phase, regardless of the state of colimation of a beam, which can be a problem with certain interferometers. If the beam is not collimated, the plate always introduced negative OPD corresponding to positive longitudinal defocus. Reference to Fig. 19 explains the sign convention. Defocus can be derived from the definition of refractive index. Light travels fastest in a vacuum, but glass is usually referenced to the speed of light in air. The refractive index is the ratio of these velocities and is always greater than one. The refractive index of air is about 1.0003, important in some cases. The focal shift caused by the plate is the difference in velocity, with and without the plate, multiplied by the time light would have taken to span the distance in a vacuum, t/c.

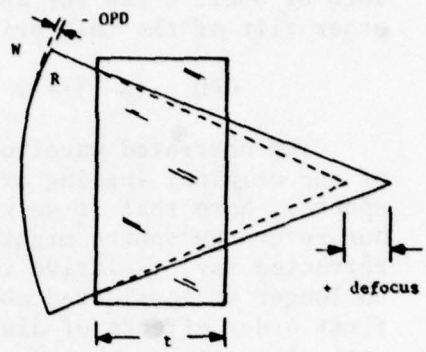

Fig. 19. Defocussing caused by disk of glass.

$$\text{Defocus} = \frac{(N - 1)}{N} t$$

Since defocussing can be converted to OPD by the previously derived expression OPD = -defocus/(8 f/#^{2}), we obtain:

$$\text{OPD} = \frac{\frac{1-N}{N} t}{8 (f\#)^2}$$

3.15 PLANE-PARALLEL GLASS PLATE: BORESIGHT

Tilting a plate in a non-collimated beam causes a boresight error, but not first-order defocussing. Referring to Fig. 20, we derive this boresight error. Note as always, we retain our reference sphere on the continuation of the original axis.

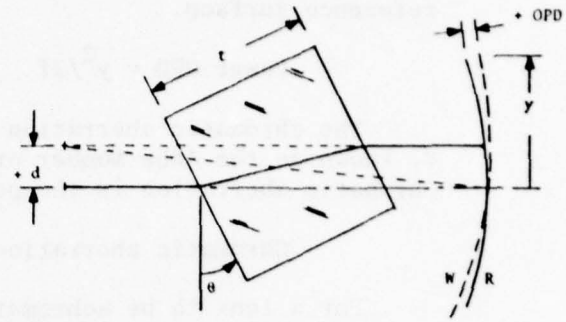

Fig. 20. Boresight error caused by tilted disk of glass.

$$d = \frac{N-1}{N} \cdot \theta \cdot t$$

$$OPD = \frac{d}{s} \cdot y$$

where s is the separation between the object point and the reference sphere

let $u' = \frac{y}{s}$, marginal ray angle of the beam

then $OPD = \frac{(N-1)}{N} \cdot \theta \cdot t \cdot u'$

or $OPD = (N-1) \cdot \theta \cdot t \cdot u$

where u is now measured inside the glass.

In terms of the local f/#, we also have,

$$OPD = \frac{(N-1) \cdot \theta \cdot t}{2 \cdot N \cdot (f/\#)}$$

3.16 CHROMATIC ABERRATION

The power of a lens can be written in wave form, using a plane reference surface.

$$\text{Power OPD} = y^2/2f$$

The chromatic aberration of a lens is defined with the quantity V, known as the Abbe Number or reciprocal dispersive power. The chromatic aberration is the power OPD divided by the Abbe Number.

$$\text{Chromatic aberration OPD} = y^2/2fV$$

For a lens to be achromatic, the sum of chromatic aberration contributions must total approximately zero. For a thin achromatic doublet, we see that,

$$f_a V_a = - f_b V_b$$

For chromatic stability, this should remain reasonably valid over a range of temperature. J. W. Perry (1943) calculated the temperature dependence of chromatic aberration for some simple lenses over a 50°C range and found good stability. An examination of Fig. 30 for BK7 glass indicates this material, at least, will be quite stable in regard to chromatic OPD. On the whole, glasses have the proper tendency to allow chromatic correction over a range of temperature. Whether there are penalties associated with picking matched glasses remains to be determined.

Differentiation of the equation leads to an intractible analytical statement of the detailed requirements. The problem is probably better handled by generating more combinations of the available glass data to facilitate predesign layout of chromatically athermal lenses.

3.17 "DECENTERED" SPHERICAL ABERRATION

The ultimate precision attainable with a boresighting instrument, apart from its mechanical refinements, is one or more orders of magnitude finer than what we would imagine from calculating its diffraction-limited resolution. Boresighting is a null technique and involves determining the "photometric" center of a presumably symmetric point image. Naturally, there are many ways in which this symmmetry may be disturbed. Some are blatant; for example, failure to illuminate the entire aperture of the instrument. Others are more insidious, an example being the use of an off-axis paraboloid to test different sensors. The paraboloid might be perfect enough to insure resolution requirements are met, yet by departing from the optical axis, an effect known as the Offense Against the Sine Condition will cause a defect in the illumination of the sensor. Furthermore, slight zonal spherical aberration in the mirror can generate additional boresight error.

The manner in which low order aberration, such as focus and boresight, can derive from higher aberrations is usually of little interest in ordinary situations, but for precision boresighting and focussing, it merits consideration. We consider an optical element

which has spherical aberration and is located at the aperture stop of the instrument. The corrector plate of a Schmidt telescope is an example. If it is perfectly aligned and the aperture fully illuminated, the telescope will show a perfectly symmetrical point spread function. Even if the corrector is imperfectly cancelling spherical aberration, the point spread function will maintain symmetry for such is the nature of spherical aberration. Now, suppose the corrector is decentered a slight amount. The new aberration appearing on the optical axis will equal the difference between the spherical aberration W centered on axis and that displaced a small distance, Δ. The apparent aberration generated on axis can be described by the series,

$$W' = W \left(4\rho^3\Delta' + 6\rho^2\Delta'^2 + 4\rho\Delta'^3 + \Delta'^4 \right)$$

where ρ is the normalized radius of the pupil,

and $\Delta' = \frac{2\Delta}{D}$, D being the diameter of the pupil.

The first term in parentheses is coma, leading to a lopsided point image. The second term describes astigmatism, effecting a focus shift. The third term is distortion, which for our purpose is indistinguishable from boresight error. The last term is a phase error, usually unimportant.

Any misalignment of an optical element tends to introduce first and higher order wave aberration. If the element has sensibly zero power, as with the Schmidt corrector, the effect is almost entirely due to sheared spherical aberration. In most optical systems, element misalignment has a far more profound effect directly on first order boresight and focus, and restraining the first order error will generally insure that terms arising from the higher order aberration are negligible.

3.18 RAYTRACE TEST OF THEORY

A retationally symmetric, mock optical design was laid out to test our methods. The design is mathematically valid, but physically unrealizable owing to extreme obstructions of the light path caused by several mirror elements. The design is suggested by Fig. 21, in which we have decentered elements to make the light path clearer. Table 1 is an exact specification of the nominal layout, in millimeters. No effort was made to correct the fourth and higher order aberrations of the design. It shows significant spherical aberration, and when elements are tilted, astigmatism is obtained on the reference axis. However, as expected, the higher aberrations are much weaker than first order defocussing and boresight which we want to test with our design.

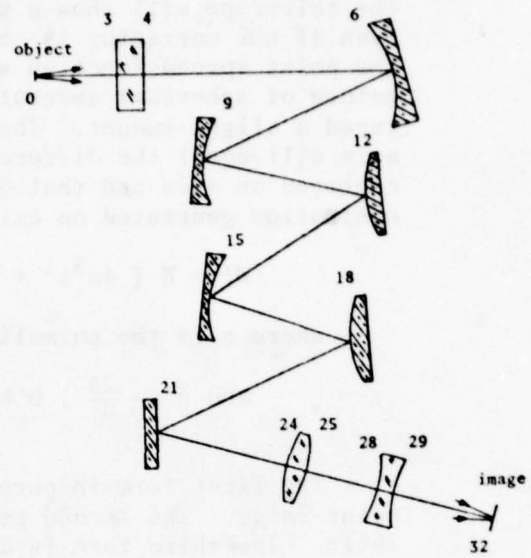

Fig. 21. Conceptual layout and surface numbering of design used to test OPD theory.

Each power surface was individually tilted and decentered by 0.1 degree and 1.0mm respectively, raytraced, reset to zero, and the process continued from the first element to the last. The tilted and decentered array was raytraced with a central ray, whose angular orientation and decentration relative to the nominal centerpoint at the focal plane was exactly determined. We also examined the astigmatism at the centerpoint to be aware of its possible influence on our test.

Each radius of curvature was changed by about 25-50 waves, the disturbed design raytraced and the focus found by using a paraxial height solve set to zero. The shift from the nominal back focal distance was thus determined. The disturbed radius was set back to nominal and the process repeated one surface after another to the end.

The refractive index of the plate and the two lenses was changed by 0.1, approximately 100 times the typical refractive index error we would encounter with optical glass. The plate was tilted and by raytrace, the boresight error was found at the final focal surface.

Each thickness was changed by 1mm and the same procedure was followed. The computer analysis resulted in approximately 250 pages of output which was checked for keypunch errors and reasonability of the analyses. The predicted wave aberration, using paraxial raytrace values for the y-heights, were converted into transverse boresight error and longitudinal defocus at the final focal plane. These predicted errors were compared with raytraced errors.

Boresight was found to be more accurately predicted, with an agreement, for this design, of about 1% with 1000 waves of predicted OPD. For radius, thickness, refractive index, and airspace errors, the accuracy was poorer: about 2% for predicted defocus on the order of 50-100 waves. Part of this inaccuracy can be attributed to the fact that a defect in the parameter changes the first order focal length and numerical aperture of the optical system, so our conversion factors should probably be scaled to reflect this change. We did not invoke this correction factor.

The relative accuracy of first order prediction as determined from exact raytracing, will depend considerably on the details of the optical design being studied. Very large boresight errors will induce central coma and central astigmatism that add higher order terms to the computed value, while changes in the

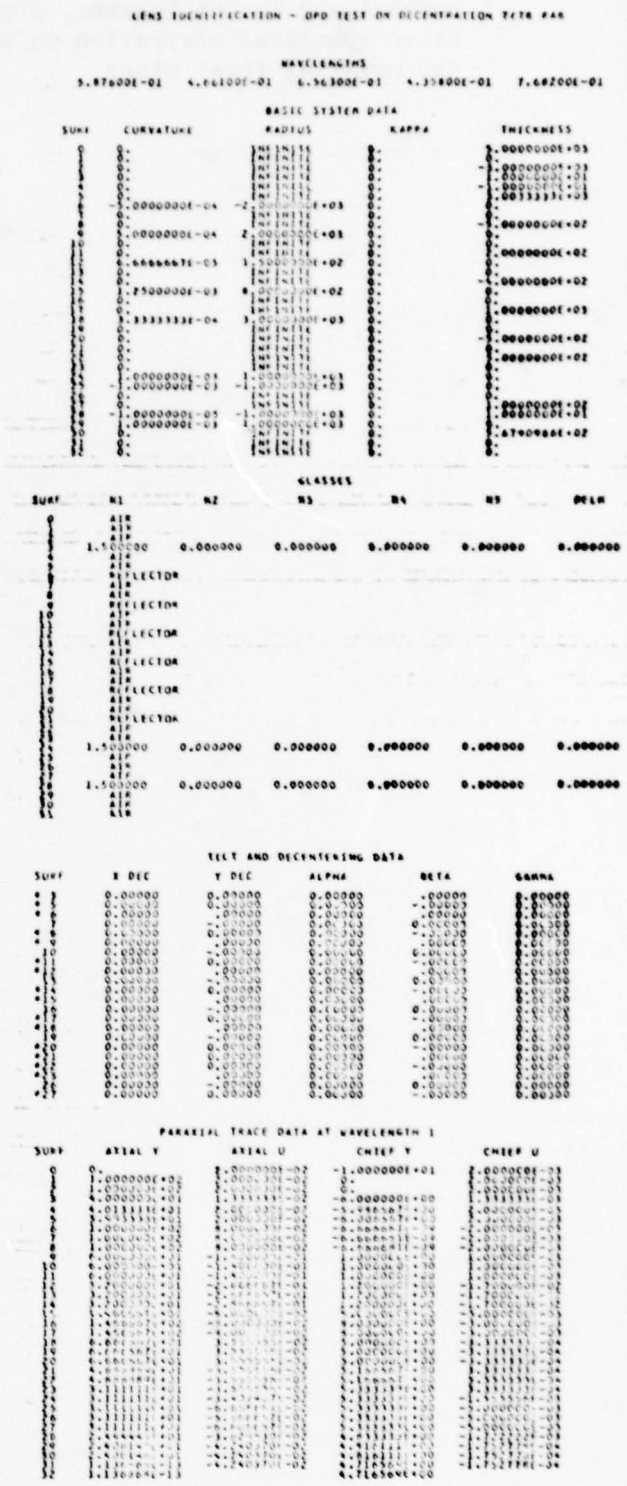

Table 1. Specification of optical design used to test OPD theory.

nominal radii, thicknesses, airspaces and refractive indices may cause spherical aberration to shift the plane of best focus from the paraxial focal plane.

4. OPTICAL MATERIALS

4.1 DISCUSSION

A wide variety of materials can be used to refract, reflect, disperse, filter, and polarize light. This section offers selection of materials which are widely used for refraction and reflection of visible light.

All things being equal, a preferred material will be durable, isotropic, and comparatively inexpensive. However, lacking alternatives, the designer takes what he can get. For the infrared, this occasionally results in using water soluable crystals, whose permanence relies on maintaining a controlled thermal and atmospheric environment.

There is a continuing development of all-reflective systems which avoid the complications of absorption and thermal distortion. We feel that this will have an important bearing on the development of improved thermal resistance in precision instrumentation.

4.2 DIELECTRIC FILTERS

Interference films, for filters, antireflection, or enhanced reflectivity, consist of dielectric layers of materials whose refractive indices alternate. Each layer has its own coefficient of expansion and variation of refractive index with temperature. Some instruments use narrow, high-efficiency stacks as bandpass filters. Exposed to excessive temperature change, these will act as cutoff filters instead. Figures 22 and 23 show some data provided by OCLI.

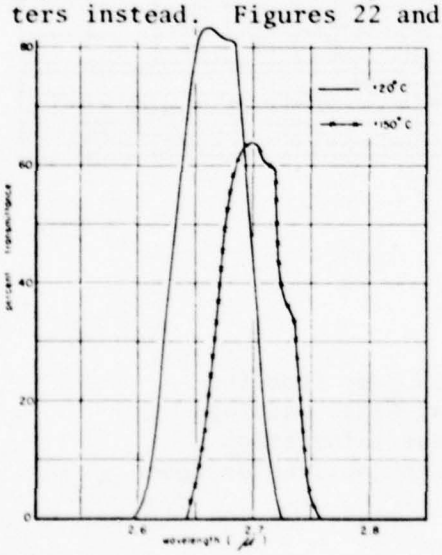

Fig. 22. Measured variation of a typical filter with temperature.

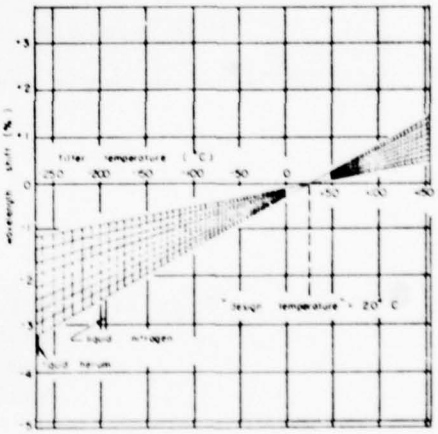

Fig. 23. Wavelength shift as a function of temperature.

4.3 OPTICAL GLASS

A modern glass catalog is actually a technical compendium of virtually every glass property likely to interest the average lens designer and mechanical engineer. One of the most highly regarded catalogs is that of the Schott Glass Company, and Fig. 24 reproduces the page which describes borosilicate glass type BK7. Figures 25 through 30 detail further information obtained from the Schott catalog. Additional material obtained from a published report will be found on Figs. 32-34 in Chapter 5.

BK 7 - 517642

			Refractive Indices for λ (nm)												
			1014.0	852.1	706.5	656.3	643.8	589.3	587.6	546.1	486.1	480.0	435.8	404.7	365.0
Refractive Index	n_d	1.51680	n_t	n_s	n_r	n_C	$n_{C'}$	n_D	n_d	n_e	n_F	$n_{F'}$	n_g	n_h	n_i
$\frac{n_d - 1}{n_{F'} - n_{C'}} - \nu_d$		64.17	1.50731	1.50581	1.51289	1.51432	1.51472	1.51673	1.51680	1.51872	1.52238	1.52283	1.52669	1.53024	1.53626
Dispersion	$n_{F'} - n_{C'}$	0.008054													
			Relative Partial Dispersions												
Refractive Index	n_e	1.51872	$\frac{n_s - n_t}{n_{F'} - n_{C'}}$ 0.3097	$\frac{n_r - n_s}{n_{F'} - n_{C'}}$ 0.3833	$\frac{n_C - n_r}{n_{F'} - n_{C'}}$ 0.1774	$\frac{n_d - n_C}{n_{F'} - n_{C'}}$ 0.3075	$\frac{n_e - n_d}{n_{F'} - n_{C'}}$ 0.2386	$\frac{n_F - n_e}{n_{F'} - n_{C'}}$ 0.4039	$\frac{n_g - n_F}{n_{F'} - n_{C'}}$ 0.5350	$\frac{n_h - n_g}{n_{F'} - n_{C'}}$ 0.4413	$\frac{n_i - n_h}{n_{F'} - n_{C'}}$ 0.7478
$\frac{n_e - 1}{n_{F'} - n_{C'}} - \nu_e$		63.96													
Dispersion	$n_{F'} - n_{C'}$	0.008110	$\frac{n_s - n_t}{n_{F'} - n_{C'}}$ 0.3075	$\frac{n_r - n_s}{n_{F'} - n_{C'}}$ 0.3806	$\frac{n_C - n_r}{n_{F'} - n_{C'}}$ 0.2252	$\frac{n_d - n_C}{n_{F'} - n_{C'}}$ 0.2565	$\frac{n_e - n_d}{n_{F'} - n_{C'}}$ 0.2370	$\frac{n_F - n_e}{n_{F'} - n_{C'}}$ 0.5065	$\frac{n_g - n_F}{n_{F'} - n_{C'}}$ 0.4755	$\frac{n_h - n_g}{n_{F'} - n_{C'}}$ 0.4380	$\frac{n_i - n_h}{n_{F'} - n_{C'}}$ 0.7427

Constants of Dispersion Formula

A_0	A_1	A_2	A_3	A_4	A_5
2.2718929	$-1.0108077 \cdot 10^{-2}$	$1.0592509 \cdot 10^{-2}$	$2.0816965 \cdot 10^{-4}$	$-7.6472538 \cdot 10^{-5}$	$4.9240991 \cdot 10^{-6}$

Deviation of Relative Partial Dispersions Δ P from the "Normal Line"

$\Delta P_{C,t} = \Delta \frac{n_C - n_t}{n_{F'} - n_{C'}}$	$\Delta P_{C,s} = \Delta \frac{n_C - n_s}{n_{F'} - n_{C'}}$	$\Delta P_{F,e} = \Delta \frac{n_F - n_e}{n_{F'} - n_{C'}}$	$\Delta P_{g,F} = \Delta \frac{n_g - n_F}{n_{F'} - n_{C'}}$	$\Delta P_{i,g} = \Delta \frac{n_i - n_g}{n_{F'} - n_{C'}}$
0.0210	0.0083	−0.0009	−0.0006	0.0029

Temperature Coefficients of Refractive Index

Range of temperature (°C)	$\frac{\Delta}{\Delta}$ relative × 10⁶/°C: C	d	e	F	g	$\frac{\Delta}{\Delta}$ absolute × 10⁶/°C: C	d	e	F	g
−40 to −20	1.9	2.1	2.2	2.5	2.7	0.2	0.3	0.4	0.6	0.9
−20 to 0	2.3	2.4	2.6	2.9	3.2	0.6	0.7	0.9	1.2	1.4
0 to +20	2.3	2.5	2.8	3.1	3.3	1.1	1.2	1.3	1.6	1.9
+20 to +40	2.8	2.9	3.0	3.3	3.6	1.5	1.6	1.7	1.9	2.2
+40 to +60	2.8	2.9	3.0	3.3	3.6	1.7	1.8	1.9	2.2	2.5
+60 to +80	2.8	2.9	3.0	3.3	3.6	1.7	1.8	2.0	2.3	2.6

Density	Bubble quality	Resistance to climatic variations	Resistivity to staining	Coefficient of linear thermal expansion (−30° to +70°C)	Coefficient of linear thermal expansion (+20° to +300°C)	Transformation temperature	Mean specific heat	Thermal conductivity	Young's Modulus	Modulus of rigidity	Poisson Ratio	Special characteristics
$\frac{g}{cm^3}$	group	group	group	$\alpha \times 10^7$/°C	$\alpha \times 10^7$/°C	Tg [°C]	$\frac{cal}{g\,°C}$	$\frac{kcal}{m\,h\,°C}$	$\frac{kp}{mm^2}$	$\frac{kp}{mm^2}$	—	—
2.51	0	2	0	71	83	559	0.205 (bei 20 °C)	0.958 (bei 20 °C)	8310	3440	0.206	—

Internal Transmittance τ_i of an Average Melt

λ (nm)	290	295	300	310	320	330	340	350	360	370	380	390	400	420	440	460	480	500	540	580	620	660	700
τ_i at 5 mm thickness		0.06	0.30	0.63	0.805	0.907	0.955	0.972	0.984	0.992	0.995	0.996	0.997	0.997	0.998	0.998	0.998	0.998	0.998	0.999	0.999	0.999	0.999
τ_i at 25 mm thickness				0.10	0.34	0.61	0.79	0.87	0.92	0.96	0.975	0.982	0.984	0.98	0.989	0.990	0.991	0.991	0.993	0.994	0.995	0.995	0.995

6 (BK)

SCHOTT No. 3050 72

Fig. 24. Representative page from the Schott Optical Glass Catalog showing general information available to the optical designer.

Fig. 25. shows that as atmospheric pressure increases, refractive index coefficient also increases. Since it is customary to refer the refractive index of glass to the air in which it is surrounded, this plot is more a representation of the apparent rather than the absolute variation of refractive index. The properties of air are definitely far more sensitive than those of glass.

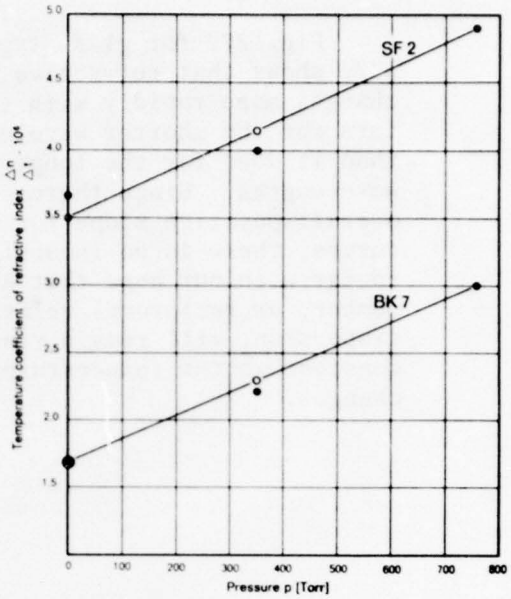

Fig. 25. Variation of refractive index thermal coefficient with variation of atmospheric pressure.

Fig. 26. will be of interest to the engineer or designer concerned with thermal gradients, and with the time glass will require to reach thermal equilibrium.

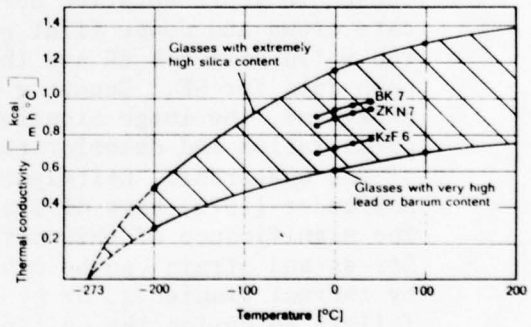

Fig. 26. Temperature effect on thermal conductivity.

Fig. 27. for glass type BK7, shows that refractive index changes more rapidly with temperature for the shorter wavelengths than it does for the longer wavelengths. Since there is an overall positive slope for all curves, there is no inconsistency so far with our hope that Abbe number, or reciprocal relative dispersion, will remain reasonably constant as the temperature changes.

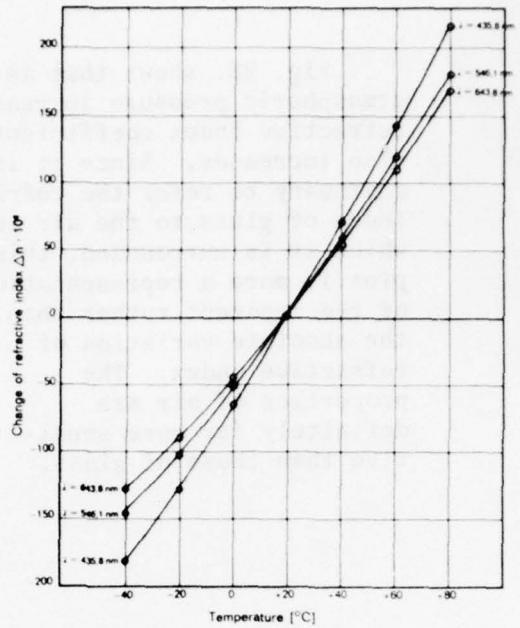

Fig. 27. Change of the refractive index of BK7

Fig. 28. shows birefringence caused in representative borosilicate crown and dense flint glass, the solid dots for BK and the open dots for SF. Behaving like a crystal, the image experiences polarization and deterioration of the wavefront. Reitmayer and Schroeder (1975) have discussed the significance of this situation. Stress and strain can be caused by thermal gradients, or by failure to design the cell properly for the range of temperature to which the instrument will be subjected.

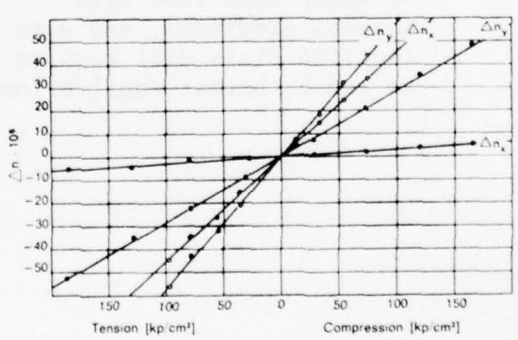

Fig. 28. Change of refractive index from compression and tension.

Fig. 29. provides additional information on the wavelength sensitivity of refractive index change for a variety of typical glasses. As explained in Chapter 3, it would be preferrable to express this data in the form of an Abbe number variation. An observation is that all the glasses in this figure behave in the same qualitative fashion.

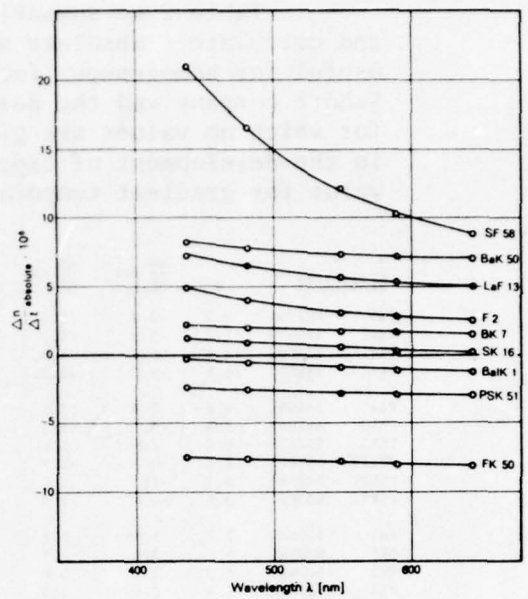

Fig. 29. Temperature coefficient of refractive index of some optical glasses.

Fig. 30. provides further insight on BK7, the most commonly used form of optical glass. The open dots pertain to refractive index measured with respect to air, the solid dots with respect to vacuum. Note that the coefficients are not constant, nor is their rate of change linear. This suggests the extreme unlikeliness that absolute thermal compensation will be possible.

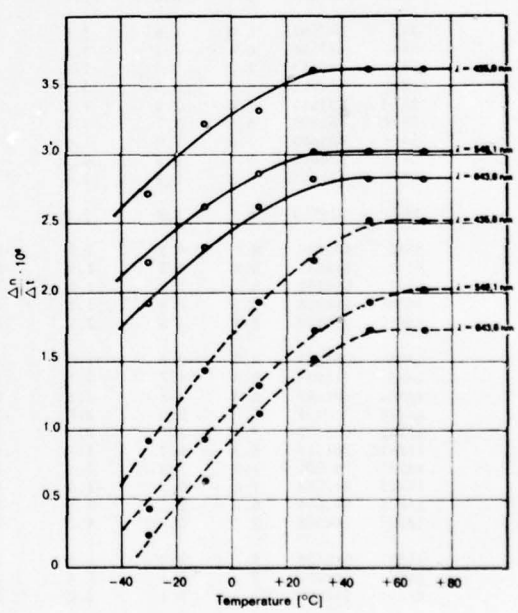

Fig. 30. Relative and absolute temperature coefficients of refractive index as functions of temperature (BK 7 glass).

In Table 2 we summarize the thermal data in the Schott catalog, and calculate absolute and relative thermal nu values which are useful for homogeneous focus. Additional data is being taken by the Schott company and the designer should inquire if he selects a glass for which no values are given. The Schott company has been engaged in the development of experimental glasses that promise to be of value for gradient temperature athermalization.

Glass Type		α	$\frac{\Delta N}{\Delta T}$ rel	$\frac{\Delta N}{\Delta T}$ abs	ν rel	ν abs
FK5	487704	9.2	-0.9	-2.3	11.0	13.9
FK6	446673	11.2	-3.9	-5.2	19.9	22.9
FKS1	487845	13.6	-6.6	-7.9	27.2	29.8
FKS2	486818	14.4	-6.5	-7.9	27.8	30.7
PK2	518651	6.9	2.9	1.5	1.3	4.0
PKS0	521697	8.8	-0.1	-1.3	9.0	11.3
PSK3	552635	6.2	2.9	1.6	1.0	3.3
PSK50	558673	8.6	-0.3	-1.7	9.1	11.7
PSK51	588683	8.3	-1.5	-2.9	10.9	13.2
PSK52	603654	8.5	-0.4	-1.9	9.2	11.7
BK1	510635	7.7	1.8	0.7	4.2	6.3
BK4	500658	6.5	2.6	1.3	1.3	3.9
BK5	505650	6.0	2.1	0.8	1.8	4.4
BK6	531621	7.8	2.4	1.0	3.3	5.9
BK7	517642	7.1	2.9	1.6	1.5	4.0
BALK1	526600	9.1	0.4	-1.1	8.3	11.2
K3	518590	8.3	2.0	0.6	4.4	7.1
K4	519574	7.3	3.5	2.4	0.6	2.7
K5	522595	8.2	1.6	0.5	5.1	7.2
K10	501564	6.5	4.1	2.8	1.7	0.9
K11	500614	6.4	3.4	2.3	-0.4	1.8
K50	523602	7.0	3.8	2.4	-0.3	2.4
K51	505596	4.3	6.6	5.3	-8.8	-6.2
BAK4	569561	7.0	3.8	2.4	0.3	2.8
BAK5	557587	7.8	1.9	0.5	4.4	6.9
BAK50	568580	3.7	8.6	7.2	-11.4	-9.0
SK2	607567	6.0	4.6	3.0	-1.6	1.1
SK4	613586	6.4	2.7	1.2	2.0	4.4
SK5	589613	5.5	3.7	2.3	-0.8	1.6
SK9	614552	6.0	5.0	3.5	-2.1	0.3
SK10	623569	7.0	2.6	1.2	2.8	5.1
SK12	583595	6.4	3.1	1.6	1.1	3.7
SK14	603606	6.0	2.8	1.4	1.4	3.7
SK16	620603	6.3	1.8	0.3	3.4	5.8
SK51	621603	8.9	-0.9	-2.4	10.3	12.8
KF2	526510	8.5	3.4	2.0	2.0	4.7
SSK2	622532	6.2	4.3	3.3	-0.7	0.9
SSK3	615512	6.6	4.3	1.9	-0.4	3.5
SSK4	618551	6.1	3.0	1.6	1.2	3.5
SSKN8	618498	7.1	2.7	1.2	2.7	5.2
SSK52	658509	6.7	3.5	2.1	1.4	3.5
LAK3	694535	8.2	-0.5	-2.0	8.9	11.1
LAK8	713538	5.6	4.7	3.1	-1.0	1.3
LAKN9	691547	6.3	3.8	2.3	0.8	3.0
LAK10	720504	5.7	5.0	3.6	-1.2	0.7
LAK11	658573	7.2	1.0	-0.5	5.7	8.0
LAKN16	734517	5.3	6.2	4.7	-3.1	-1.1
LAK17	788505	5.9	3.9	2.3	1.0	3.0
LAK25	691548	7.9	-0.3	-1.8	8.3	10.5
LAK26	692586	6.9	1.2	-0.3	5.2	7.3
LAK28	744508	5.7	5.7	4.2	-2.0	0.1
LLF1	548458	8.1	3.0	1.6	2.6	5.2
LLF4	561452	8.2	2.6	1.4	3.6	5.7
LLF6	532488	7.5	3.4	2.0	1.1	3.7
BAF4	606439	7.9	3.6	2.2	2.0	4.3
BAF9	643480	6.5	5.1	3.7	-1.4	0.7
BAF52	609464	8.4	1.8	0.4	5.4	7.7
BAF53	670471	6.5	4.4	3.0	-0.1	2.0
BAF54	667482	6.2	4.5	3.1	-0.5	1.6
BALF4	580537	6.4	5.2	3.8	-2.6	-0.2
BALF6	589530	6.7	4.1	2.9	-0.3	1.8
BALF8	554512	8.3	2.3	0.8	4.1	6.9
BALF50	589514	8.3	1.3	-0.1	6.1	8.5
BALFS1	574521	8.1	2.1	0.7	4.4	6.9
LF1	573426	8.5	2.4	1.1	4.3	6.6
LF5	581409	9.1	2.6	1.2	4.6	7.0
LF8	564438	8.5	2.2	0.8	4.6	7.1
F1	626357	8.7	3.4	1.8	3.3	5.8
F2	620364	8.2	3.9	2.8	1.9	3.7
F3	613370	8.0	4.6	3.1	0.5	2.9
F4	617366	8.3	3.7	2.4	2.3	4.4
BASF5	603425	7.9	9.7	8.3	-8.2	-5.9
BASF55	700347	5.1	8.8	7.3	-7.5	-5.3
BASF56	657367	8.1	4.9	3.4	0.6	2.9
BASF57	651419	7.1	4.7	3.3	-0.1	2.0
LAFN2	744448	8.2	1.9	0.3	5.6	7.8
LAF13	776378	5.7	6.9	5.3	-3.2	-1.1
LAF21	788474	5.9	4.9	3.3	-0.3	1.7
LAF25	784413	5.8	8.1	6.5	-4.5	-2.5
LASF5	881410	5.9	5.1	3.3	0.1	2.2
LASF9	850322	7.6	4.2	2.6	2.7	4.5
LASF12	836423	6.0	5.3	3.6	-0.3	1.7
LASF13	855366	6.2	9.3	7.6	-4.7	-2.7
LASF15	878382	6.3	5.6	3.9	-0.1	1.9
SF1	717295	8.1	7.4	5.8	-2.2	0.0
SF2	648339	8.4	4.5	3.1	1.5	3.6
SF3	740282	8.4	7.5	5.9	-1.7	0.4
SF4	755276	8.0	8.9	7.3	-3.8	-1.7
SF5	673322	8.2	5.7	4.2	-0.3	2.0
SF6	805254	8.1	10.3	8.6	-4.7	-2.6
SF8	689312	8.2	7.4	5.6	-2.5	0.1
SF10	728284	7.5	7.6	6.0	-2.9	-0.7
SF12	648338	7.8	5.3	3.8	-0.4	1.9
SF19	667330	7.7	6.0	4.5	-1.3	1.0
SF50	655329	10.1	2.0	0.6	7.0	9.2
SF54	741281	7.7	8.1	6.5	-3.2	-1.1
SF55	762270	8.2	7.8	6.3	-2.0	-0.1
SF56	785261	7.9	7.3	5.7	-1.4	0.6
SF58	918215	9.0	12.4	10.3	-4.5	-2.2
SF61	751275	7.9	8.1	6.5	-2.9	-0.8
SF62	681319	8.2	6.1	4.6	-0.8	1.4
SF63	748277	8.2	7.9	6.4	-2.4	-0.4
TIK1	479587	10.3	-2.3	-3.6	15.1	17.8
KZF1	551497	6.9	3.9	2.5	-0.2	2.4
KZF2	529517	6.0	4.3	2.9	-2.1	0.5
KZF5	521527	5.7	3.7	2.4	-1.4	1.1
KZFSN4	613443	4.5	5.2	3.7	-4.0	-1.5
KZFS6	592485	5.1	3.9	2.5	-1.5	0.9
KZFS7	681374	5.3	4.4	2.9	-1.2	1.0
KZFS8	720346	5.3	7.5	6.0	-5.1	-3.0
KZFS9	599470	5.1	3.7	2.3	-1.1	1.3
LGSK2	586610	12.1	-3.1	-4.5	17.4	19.8

Table 2. Thermal properties of Schott Optical Glass

4.4 PLASTICS

Plastic is still trying to live down a bad reputation given it by early workers in the field. Most plastic lenses were, and some still are, produced with the same machinery, tooling, and time-pressure-temperature cycling used to produce ordinary mechanical parts. Obviously, plastic will never have the intrinsic stability and amenability to surface accuracy as optical glass, but companies such as Kodak, Polaroid, Bell & Howell, Consolidated Optical Industries, and MU Engineering are demonstrating the feasibility plastic lenses replacing glass in many difficult applications. Although manufacturers are reluctant to certify the repeatability of optical properties from batch to batch, private communications indicate that in fact plastic is already produced with a high degree of repeatability without special attention. This would seem logical for a single constituent compound such as acrylic, but is more dependent on quality control for copolymers.

The advantages of plastic are its low cost, light weight, and its ability to be molded to finished shape and surface quality for a great cost advantage. An important but apparantly unresearched technical advantage is that all the plastics for which we have data show negative Gamma coefficients. Only a few glasses have negative values, so athermalization for radial gradients should be easy if some plastic is deliberately included in an otherwise all-glass design. The reader is warned that some published literature gives the incorrect sign for refractive index variation.

Most plastic lenses are made from acrylic and polystyrene, although Kodak and Polaroid have concocted special mixes to obtain particular advantages. The polycarbonates, more difficult to injection mold, are desirable for their higher softening temperature. Table 3 summarizes such data as are commonly available on plastics used in lenses.

Plastic	N_D	V_D	$\frac{\Delta N}{\Delta T}$ ($10^{-6}/^oC$)	α ($10^{-6}/^oC$)
1. Poly (methyl methacrylate)	1.490	57.8	-90	83
2. Poly (ally diglycol carbonate) "CR39"	1.498	59.0	-140	138
3. Polystyrene	1.591	30.9	-120	75
4. Polyvinyl toluene	1.580	31.4	-220	91
5. Epoxy (DOW QX2444)	1.548	39.3	-100	60
6. Polycarbonate "Lexan"	1.585	30.2	---	60
7. Polymethyl pentene "TPX"	1.467	52	---	117
8. Styrene acrylonitrile "SAN"	1.563	34.5	---	66
9. Polysulfone	1.633	---	---	56
10. Fluorocarbons	1.34 -1.44	---	---	150-70

Table 3. Selected plastic materials for optical lens elements.

4.5 FLUIDS

Any transparent substance is potentially useful for optical purposes. The first microscope, constructed almost 350 years ago by Leeuwenhoek, used a drop of water as its lens. Although Dolland is credited with the first practical achromat, experiments with dispersive fluids, in lieu of flint glass, preceded it. Today, designers find fluids useful for coupling dissimilar materials, for conducting the heat away from high intensity CRT faceplates, for filtration, for image stabilizers, and for hybridization with injection molded aspheric plastic shells to produce low-cost high aperture projection lenses.

Any fluid used for optical purposes should ideally be nonflammable and nontoxic, but special applications warrant special risks. Some of the fluids for optical design are indicated in Table 4.

Fluid	N_D	V_D	Volume Expansion ($10^{-3}/^{o}C$)
1. Acetone	1.359	54	1.487
2. Methyl alcohol	1.329	61	1.199
3. Benzene	1.501	30	1.237
4. Carbon disulphide	1.628	18	1.218
5. Carbon tetrachloride	1.461	48	1.236
6. Ethyl ether	1.354	58	1.656
7. Glycerine	1.473	61	0.505
8. Mercury	---	--	0.19175
9. Olive oil	1.476	55	0.721
10. Petroleum, density .8467	1.516	55	0.955
11. Turpentine	1.472	47	0.973
12. Water	1.333	56	0.207

Table 4. Selected fluids for optical applications.

4.6 MIRROR SUBSTRATES

All rotationally symmetric reflective optical systems have central obstructions that reduce transmission and expand the diffraction image. Asymmetrical reflectors exhibit polarization and generally have slightly imperfect diffraction point spread functions due to anamorphosis and aberration of the exit pupil. Apart from this, most designers would approve wholeheartedly of using reflective designs in lieu of refractors.

Whenever thermal gradients are anticipated, zero expansion materials are preferred. Even CER-VIT, though, in not perfect as may be seen in Fig. 31. As far as we know, there is no such thing as a perfectly stable material.

Provided absolute thermal isotropy can be assured, easy athermalization of focus and boresight is obtained simply by making the cell structure as well as the mirrors from the same material. Although the focal length will change, a temperature change scales the entire design and the image remains in focus. Thus, an all-aluminum telescope has some advantages if it can be shielded from the sun. High conductivity alone is not sufficient to preclude gradients, only reduce them.

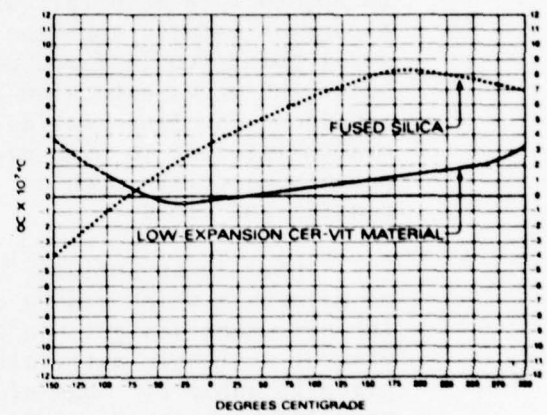

Fig. 31. Thermal expansion of CER-VIT compared with ordinary fused silica.

Table 5 compiles data on some of the more widely used mirror substrate materials. For special purposes, germanium and silicon are useful as mirrors. It is understood that the substrate is usually given a reflective coating of some metal.

Material	ρ Density gm/cm^3	E Modulus of Elasticity $10^6 N/cm^2$	K Thermal Conductivity cal/cm-sec-°C	C Specific Heat cal/gm°C	α Coefficient of Expansion $10^{-6}/°C$	Specific Stiffness E/ρ $10^6 cm$	Thermal Diffusivity D- $K/C\rho$
Pyrex	2.23	6.7	0.0027	0.18	3.25	3.0	0.007
Fused Silica	2.2	7.0	0.0033	0.188	0.55	3.18	0.008
ULE	2.21	6.74	0.0031	0.183	0.0	3.05	0.008
Cer-Vit	2.5	9.23	0.004	0.217	0.0	3.7	0.008
Aluminum	2.70	6.9	0.53	0.215	23.9	2.56	0.92
Beryllium	1.83	28.0	0.38	0.45	12.4	15.4	0.46
Graphite/Epoxy	1.72	6.9	0.12	0.24	0.03	4.0	0.29

Table 5. Properties of Selected mirror substrate materials.

4.7 MECHANICAL MATERIALS

Optical elements must be supported and housed with great precision, and this is accomplished by mechanical design which respects thermal influence on the optical design. The arbitrary choice of zero expansion cell materials is naive indeed, if not excessively expensive. The materials selected might be mainly based on weight considerations. Most lenses are mounted in aluminum whether this be good for them or not. The elements must then be spaced with materials whose expansion insures that the focal point remain fixed despite the great expansion of aluminum. We find considerable interest in high expansion materials such as plastic and fluid.

There is an infinite variety of materials which can be used in instrument design. An overview of available materials is given in Table 6. Some of the more interesting materials include machineable ceramics and filled resins. Injection molded plastic parts are worthy of consideration.

Material	α ($10^{-6}/^{o}C$)
1. Silicone rubber	810
2. Rubber and elastomers	700-480
3. "plastics", including filled and reinforced	300-0
4. Zinc, alloys	35-10
5. Magnesium, alloys	29-25
6. Aluminum, alloys	24-12
7. Copper, alloys	21-16
8. Irons	19-11
9. Stainless steels	19-10
10. Steels	15-10
11. Nickel, alloys	17-0
12. Beryllium, alloys	16-11
13. Titanium, alloys	11-7
14. Glass	15-3
15. Carbon & graphite, composites	8-1
16. Ceramics	7-0
17. Molybdenum, alloys	6-5
18. Tungsten	4
19. Ultra-low expansion glasses, alloys, miscellaneous	0

Table 6. Thermal expansion of selected materials useable for mechanical elements.

5. DESIGN TECHNIQUES

5.1 DISCUSSION

The purpose of this section is to discuss some of the known ways to athermalize or desensitize an optical system. We deal mainly with homogeneous temperature change since this is the only area that has been researched in depth. The case of thermal gradients in complex systems is very difficult and is discussed conceptually. Athermalization is ripe for invention, and some of the better ideas are based on scientific logic and common sense rather than any detailed understanding of optical materials and elaborate formulations. The reader should consider the approaches described herein only in introduction to the subject.

5.2 ACHROMATIC LENS

This topic is well treated by Perry (1943), Grey (1948), and Kohler and Strahle (1972). To summarize, the focal length of an individual thin element is athermalized for homogeneous changes when is thermal nu value is zero, where nu is defined as:

$$\nu = \frac{\frac{\Delta N}{\Delta T}}{(N-1)} - \alpha$$

The individual element is unaffected by radial gradients if instead its Gamma value is zero, where Gamma is defined as:

$$\Gamma = \frac{\frac{\Delta N}{\Delta T}}{(N-1)} + \alpha$$

Note that the two requirements are mutually exclusive unless both the expansion coefficient and the refraction coefficient are zero. No such glass is known, indeed, materials such as fused quartz, with a very low expansion coefficient, seem to have unusually high refractive index coefficient.

Figs. 32 and 33, taken from Kohler and Strahle, are valuable for picking out attractive glass choices. Note there are almost no glasses with a zero or negative Gamma. Plastic, on the other hand, abounds in large negative Gammas, and should thus be useful in designing lenses insensitive to radial gradients if combined with optical glass.

The design of an achromatic doublet is amenable to simple analysis. First, the pair must satisfy the usual requirements on component focal length versus Abbe number:

$$f_a = f(V_a - V_b)/V_a$$

$$f_b = f(V_b - V_a)/V_b$$

Second, for athermalization under homogeneous temperature change, we should also satisfy the condition,

$$V_a \nu_a = V_b \nu_b$$

Fig. 34. was designed for this purpose. Finally, if we want our doublet to show radial gradient insensitivity, we must satisfy the condition,

$$0 = \sum (N-1) \cdot t \cdot \Gamma$$

where t is the element thickness. As with a singlet, it appears impossible to make our doublet insensitive to both homogeneous and gradient temperatures.

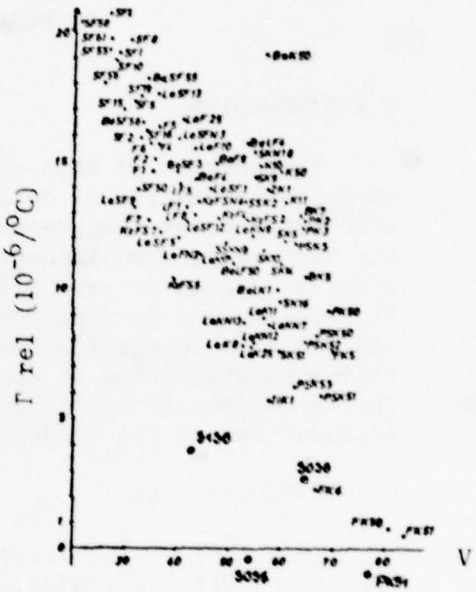

Fig. 32. Data for homogeneous temperature athermalization.

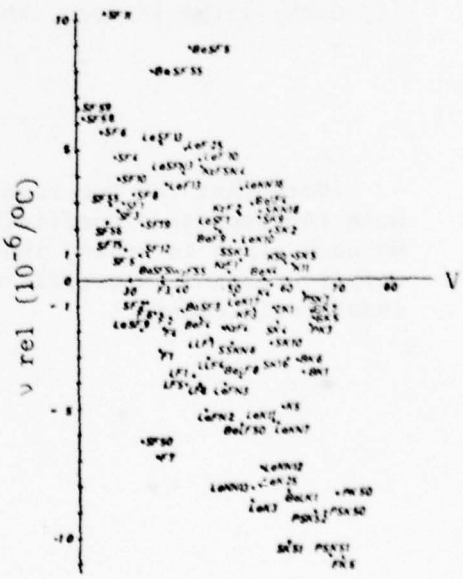

Fig. 33. Data for radial gradient athermalization.

Apart from the work reported by Kohler and Strahle, we know of no serious effort being paid to glass choice for insensitivity to radial gradients. The designer will also remark that the glasses thus far indicated are the most fragile in the glass catalog, prone to break with light shock, even that caused by preparing the lens surface for antireflection coatings. We have already explained that plastic could be used to compensate the radial effects in glass, and we suggest that to be an area worthy of investigation. We also suggest the mechanical designer might design spacers responsive to thermal gradients and thereby obviate the need for complicated glass. In effect we feel the solution to the problem of radial thermal gradients has a number of choices, with new developments in glass being only one.

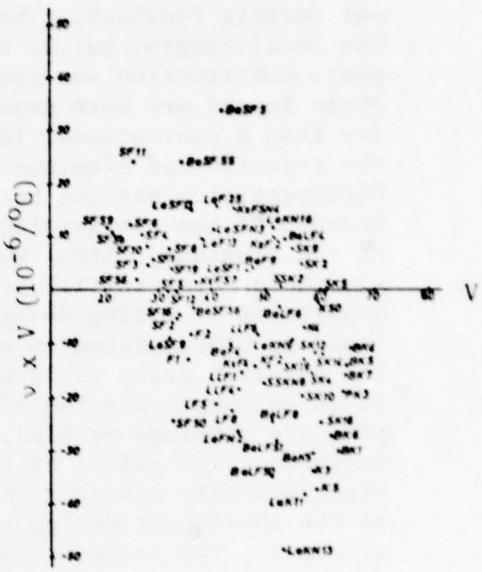

Fig. 34. Data for selecting achromatic glass pairs for athermal doublets.

The conventional method for athermalizing a lens is shown schematically in Fig. 35.

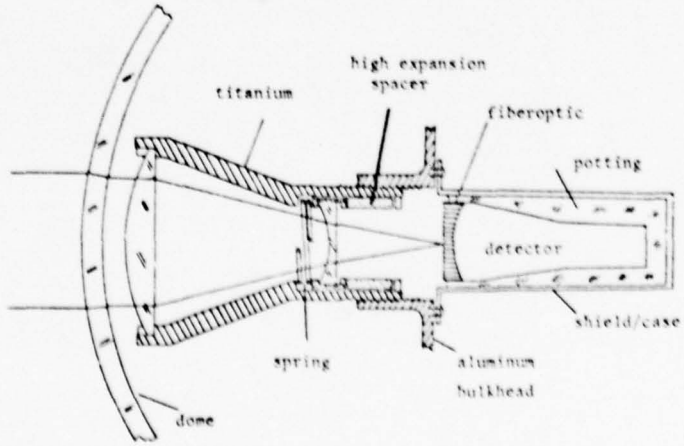

Fig. 35. Concept of focus-compensated television sensor.

The logic behind this layout follows. First, the lens exists and is used in the current Air Force television Maverick guidance unit. The operating system requires the lens remain in focus without cockpit feedback. The lens replaced an older version with half the focal length, but as no additional space was available a telephoto construction was required. A tolerance analysis showed telephoto lenses are more sensitive toward focus and centration sensitivity than a conventional lens of the same focal length. This led to the rejection of aluminum as a cell material because of excessive differential expansion between the metal and the lens diameters, and because of the exaggerated defocussing caused by longitudinal expansion of the aluminum. Steel was rejected because of its weight. Titanium was chosen over initial protests from the pricing and manufacturing departments. During design, it was established that a telephoto could be athermalized in either of two ways. First, the glass for the negative group could be chosen for an extreme rate of change, so as to compensate the effects of expansion in the forward lens group plus the combined residual effects of the titanium and the aluminum bulkhead. The effect of the vidicon shifting in its potting was experimentally measured and included in the computation. MTF analysis of the subsequent design showed it unsatisfactory at the temperature extremes. The second solution was to use a high expansion 'pusher' spacer as shown in Fig. 35. This approach is somewhat undesirable because friction can cause the spacer to bind. However, MTF analysis showed good performance over the temperature extremes, and so this was the solution used for the lens. It is worth remarking that in the end, the exact length of the plastic spacer was determined experimentally, with a variable makeup spacer of aluminum to obtain the nominal lens position. The lens has been in large scale production for several years, and the cost of the titanium cell, a major initial worry, was reduced to modest proportions by quantity production.

5.3 MIRROR FOLDS FOR STABILITY

The cube corner reflector is an interesting device. A light beam incident on it always returns in the same direction no matter how the cube corner is tilted. A single flat mirror, on the other hand, will reflect light at twice whatever angle the mirror is tilted. Is there such a thing as a "right angle cube corner"? We don't know. The next best thing is a pair of mirrors as shown in Fig. 36.

For a pair of inclined flat mirrors, light travelling parallel to the meridional plane will always leave at the same angle regardless of the angle between the mirrors and regardless of the angle the pair is tilted. The mirror system is therefore insensitive to tilts in one plane. The pentaprism is equivalent to a pair of mirrors, but has the disadvantage that it is temperature sensitive while the mirrors could be made from zero expansion material and mounted on a zero expansion holder. True, the mirror pair is not insensitive to tilts in other planes, but it is easier to design an instrument when not all degrees of freedom need restraint.

We suggest the designer can find many practical applications for the double mirror. We further suggest it is prudent to avoid the use of prisms in precision systems because of the impossibility of making a prism insensitive to both thermal gradients and homogeneous temperature changes at the same time. Furthermore, it is presently impractical for the average designer to model the effects of thermal gradients affecting refractive index as well as surface shape with light doubly traversing a pentaprism, much less some of the more complicated folding and transfer prisms that are in regular use.

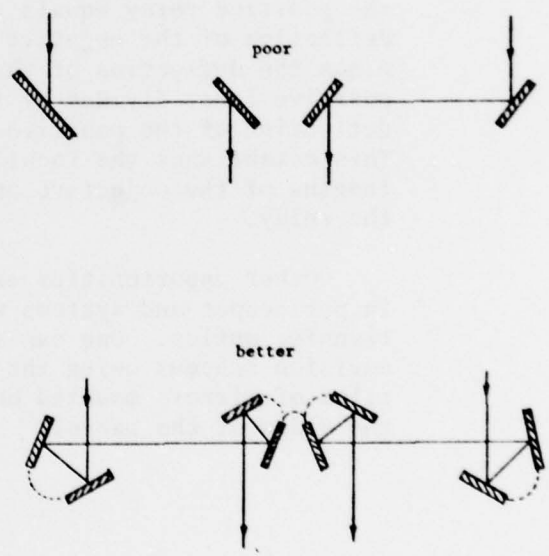

Fig. 36. Technique for maintaining parallelism of boresight axes.

5.4 OPTICAL LEVER COMPENSATION

A long barrel will bend when exposed more heat on one side than the other. Likewise, a barrel will bend when exposed to changing g-forces, vibration and so forth. The optical lever method can be used to compensate these effects.

Consider Fig. 37, where light is incident or exiting at the left. Suppose the tube is deflecting with a parabolic shape, although the method applies to any repeatable curve. Light passes through the center of the negative lens and forms a virtual focus. This is relayed by a positive lens to the final focus. If the input beam is sensibly collimated, the deflected lens motion is self compensated when the magnification of the positive relay equals the deflection of the negative lens minus the deflection of the positive lens, divided by the deflection of the positive lens. This establishes the focal lengths of the objective and the relay.

Other opportunities exist in periscopes and systems with transfer optics. One can also envision schemes using the tilts of mirrors mounted on the sides of the barrel.

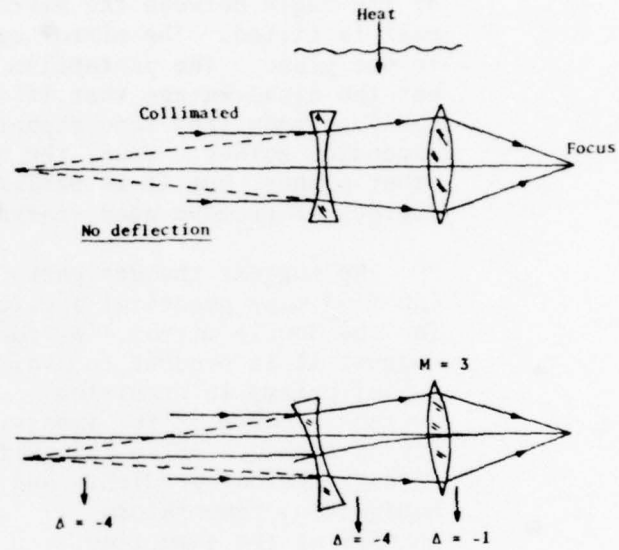

Fig. 37. Boresight stabilization using the optical lever.

5.5 INERTIAL REFERENCE

An extension of the optical lever concept is the inertially stabilized optical system. Gravity is an ideal reference for quiet, nearly stationary instruments. Gyroscopically controlled elements are completely applicable but noisy and require a power source. This section of the report is intended to provoke thought on the use of moving elements, contrary to the other school of thought which seeks to eliminate element motion as perfectly as possible.

Fig. 38. is the protoform of many image motion compensation schemes: the use of an inertially fixed or otherwise controlled mirror, with a telescopic attachment to create something near a 2:1 or 1:2 magnification to counteract the angle doubling that occurs with reflection. The mirror could be stabilized with a plumb bob, or with a gyroscopic attachment. It is perhaps worth saying that stabilizers can be used forward or backward, which is an aid in laying out new configurations.

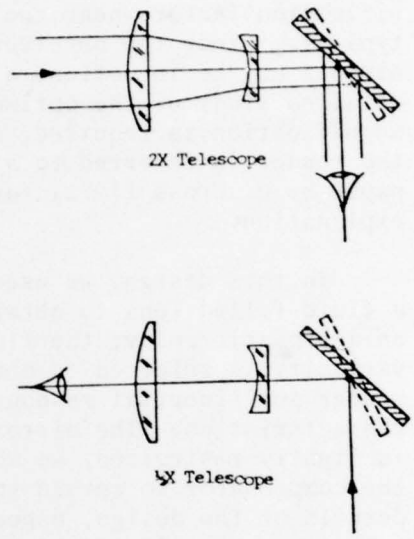

Fig. 38. Symmetrical nature of image stabilizer.

Fig. 39. shows the use of a semi-inertial reference mirror to compensate for vibrations in a hand-held telescope of moderate power. No power supply is required, yet a good damping spectrum is obtained. Many IMC schemes are similar to this one, but use a gyroscopic connection to the IMC mirror. Since mirrors double the angle of error, magnification factors near two are typical. Since the observer himself may be in motion, a detailed study of the optimum magnification is required, and the reader is referred to a paper by R. Gross (1971) for explanation.

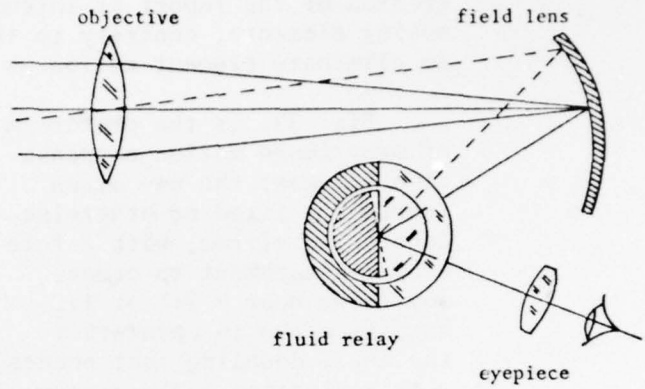

Fig. 39. Fluid-filled relay image stabilizer concept.

In this design, we used a fluid-filled lens to obtain an achromatic relay; the fluid's viscosity is selected to obtain proper semi-inertial response characteristics. The mirror is lightly restrained, so when repointed, the restoring forces permit the compensator to return to nominal axial alignment. The optical details of the design, especially image tilt and wobble during stabilization, are interesting but beyond the scope of this discussion.

Prismatic compensation lends itself to in-line layout and greater compactness. Since the refractive elements are nominally centered, they can be given curvature and serve additional use. This is not practical with reflectors because oblique incidence on other than a plane results in anamorphic aberration.

While a mirror deflects at double its tilt, a low index prism halves the angle of tilt. The idea is shown in Fig. 40, where an appropriate fluid is encased between two windows. If the instrument is vibrated, one of the windows remains inertial and forms a fluid prism. Two prisms are used. A design of this sort won an Academy Award for the Dyna-Sciences Company.

For those that are reluctant to risk the use of fluid, an all-glass equivalent is shown in Fig. 41.

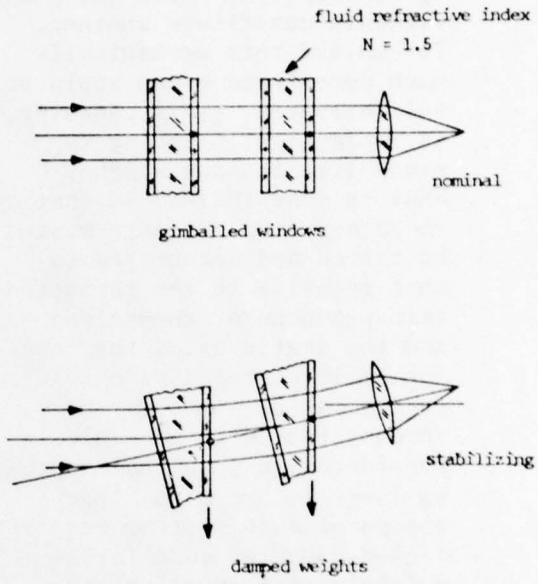

Fig. 40. Image motion compensation using fluid filled prisms.

The designer will realize that prism can be generated in more complicated ways, and Fig. 42 shows one in which only a single element need be moved. However, if there be good reason, and such reasons may pertain to the state of aberration correction, a very large number of elements may be ganged for best system performance. The point is that whenever a lens is decentered, a prismatic effect is generated which in addition to changing boresight introduces image aberration. This aberration can be compensated by decentering additional optical elements.

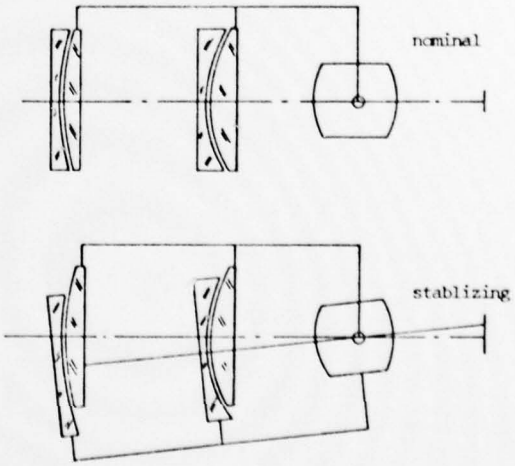

Fig. 41. Prism equivalent using lenses for image stabilization.

In fact, full correction over the field of view can be maintained during stabilization, but only if the decentered elemants consitute the equivalent of one rotationally symmetric optical system, while the static elements constitute another. To achieve this mechanically, each decentered group would be selfcorrected. This, however, is impractical, leading to excessive size and weight. What is done instead is that the decentered elements must be tilted and decentered so that relative to the refracted axis produced by themselves and the static axis, they are optically centered on a refracted axis. This may be inconsistent with mechanical considerations, so that approximations are accepted. The design of such systems requires a good computer code for multiple configuration, or zoom, elements.

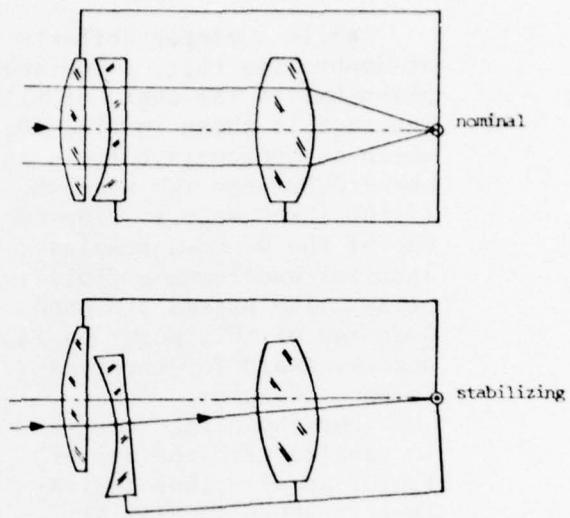

Fig. 42. Image stabilization based on lens decentration.

5.6 ZOOM LENS

Zoom lenses are placed in two classes: the optically compensated and the mechanically compensated. In the former class, groups of elements are linked together and move as a whole. In the latter, a smaller number of groups are linked by cam or computer drive and follow separate, nonlinearly related paths. Most wide range zooms are of the mechanically compensated type, and it is these that we will discuss.

The mechanically compensated zoom usually consists of three parts: a fixed objective group, a zooming relay group, and a fixed backing relay group. Errors in focus are obtained when any parameter departs from nominal. A maximum of two thermal compensator spacers will permit athermalization of focus. If no backing group is used, only one spacer is required. The problem of tolerancing a zoom for focus is essentially no different than tolerancing an ordinary fixed focus lens.

The problem of boresight is infinitely more complicated. Image runout arises from numerous sources. Two dimensional meandering of the image is due to not separating the moving groups along a perfectly straight line. One dimensional wander, which may reverse itself several times, is due to every source of tilt and decentration in the lens and its mechanical parts. The problem is aggravated by the requirement a long zoom range be packaged as compactly as possible. This makes the powers of the moving elements stronger than the overall lens focal length. As we've shown, sensitivity to defocussing is proportional to lens power. Needless to say, the tolerances needed to minimize boresight error are extreme and can lead to very complex cell design.

It is impossible to deal with every aspect of the problem, so we shall illustrate with just the decentration of lens groups in a comparatively straightforward long range zoom.

The equations governing the ralative lens motions in a mechanically compensated zoom are given below, the significance of terms being shown in Fig. 43.

$$t = \tfrac{1}{2}\left(k + \left(k^2 - 4af_1f_2 - 4k(f_1 + f_2)\right)^{\frac{1}{2}}\right)$$

$$\ell = f_1\left(\frac{k - t(1 - m)}{f_1(1 - m) + mt}\right)$$

$$\ell' = k - \ell - t$$

$$a = \frac{(1 - m)^2}{m}$$

First order equations like these are allowable in laying out a zoom, and in subsequent cam derivation, because to the first approximation, every thick optical system behaves like a thin lens provided measurements are taken relative to the principal planes. For one design, we used the values below.

$$1 \leq m \leq 10$$

$$k = +25 \text{ mm}$$

$$f_1 = +50 \text{ mm}$$

$$f_2 = -50 \text{ mm}$$

Representative solutions to the equations are given in Table 7. It is customary in designing a zoom to pick three focal lengths: the shortest, the longest, and the geometric mean. Final analysis usually allows two additional intermediate focal lengths.

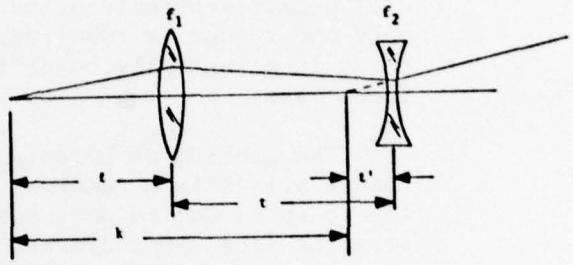

Fig. 43. Parameters of the moving elements in a mechanically compensated zoom.

M	t	t	t'
1	25.000	50.000	-50.000
2	50.000	75.00	-100.000
3	71.573	73.286	-119.859
3.1623	74.569	72.924	-122.493
4	88.535	71.178	-134.713
5	102.812	69.453	-147.265
6	115.325	68.065	-158.390
7	126.576	66.929	-168.506
8	136.873	65.982	-177.855
9	146.418	65.177	-186.595
10	155.350	64.483	-194.834

Table 7. Representative zoom Separations relative to principal planes.

Fig. 44. shows the optics at three representative magnifications. The dotted lines represent a ray perimeter and is not a raytrace. We find that providing a ray perimeter, which shows the 'stand clear' region, is a better way to communicate with the cell designer than to provide conventional raytraces.

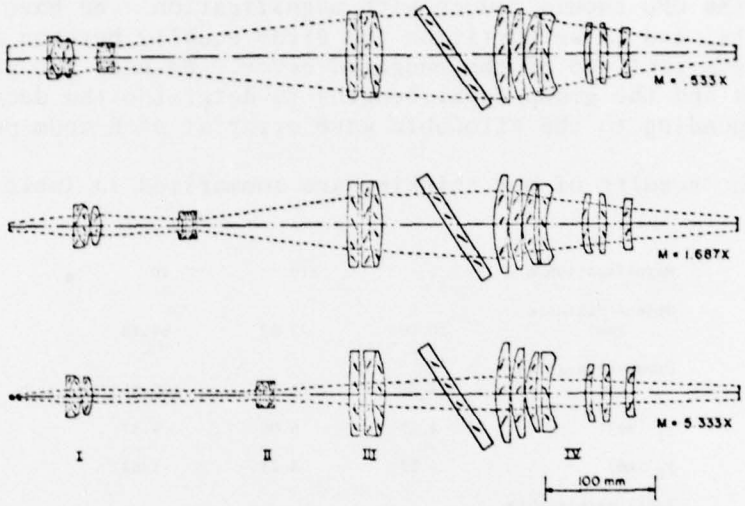

Fig. 44. Zoom Imaging Section at extreme and mean magnifications.

This lens is a relay for a fixed aperture objective. The beam of light presented to the relay is around f/6 and has a central obscuration, so we cannot put an iris in our relay.

Let us now discuss tolerances. If we want to keep a constant resolution in object space, we would specify that our zoom hold a constant OPD error over its range. But this would be foolish because then we'd magnify the image without increasing resolution. Thus, our OPD must decrease by a 10:1 range during zoom in order to maintain a fixed resolvable cell size on the detector. We may also assign a boresight tolerance on this basis. If we adjusted the lens to have a fixed output f-number, then it would be proper to tolerance the lens on the basis of fixed OPD. Most conventional zoom lenses have a fixed iris location in the backing relay and hold a constant f-number so long as the entrance aperture permits. The ultra-range new television zooms, with ranges of 30 or even 40:1, cannot maintain a fixed f-number over the whole range because the objective lens would become prohibitively large and secondary chromatic aberration intolerable. They hold f-number over a range of shorter focal length, then reduce speed at the longest focal lengths.

We can assign mechanical runout tolerances to the cells of both moving groups by using OPD theory. We require a paraxial marginal raytrace at a sampling of zoom positions, three usually being sufficient. The total error assigned to the mechanical parts is settled with an overall error budget that is based on the practicalities of lens

making versus metal working. In theory, if the lenses are adjustable in their cells, nearly the whole budget can be assigned to the mechanical mechanisms. If this mechanism is adjustable for overall centration and tilt, boresight is optimized but still susceptable to thermal expansion effects, as well as wear and friction.

We elected to hold a fixed cell size on the detector, which meant the OPD should reduce with magnification. We have two moving elements, and if we partition the error equally between the two, each gets root-two of the budgeted error. We need the paraxial ray heights and the group focal lengths to determine the decentrations corresponding to the allowable wave error at each zoom position.

The results of our thinking are summarized in Table 8.

Magnification, m	1	$\sqrt{10}$	10
Object distance (mm)	50.00	72.92	64.48
Group separation (mm)	25.00	74.57	155.35
y_1 (mm)	4.17	6.08	5.37
y_2 (mm)	4.17	3.23	1.62
Total permissable error* (waves)	2.00	0.63	0.20
Error per group = total/ $\sqrt{N}$	1.40	0.45	0.14
Permissable runout (radius) of Group I (mm)	0.010	0.0022	0.0008
Permissable runout of Group II (mm)	0.010	0.0041	0.0026

Table 8. OPD Tolerance analysis of group decentrations in sample design. (*derives from goal of .014mm image runout)

Let's consider the tolerances before we hand them over to the mechanical designer. We see that Group I reaches a runout tolerance of only .0008 mm, one wavelength of light. We know that tolerances of even .01mm are severe, particularly with moving parts. In point of fact, we had no illusion of meeting these tolerances. The customer was told before the design was initiated that a boresight runout of 2% of the frame size would constitute the best we could achieve in practice. Greater precision would come at a prohibitive price and one might as well reconcile himself to the need for feedback loops in precision boresight zoom systems.

6. CONCLUSIONS AND RECOMMENDATIONS

6.1 CONCLUSIONS

We hope we have helped make the reader feel more at ease with wave theory as applied to boresight and focus. We hope he agrees with us that this approach offers some clear insights on the source of the problem. If the reader wants to continue his study of wave theory, the text by Hopkins (1950) is recommended.

As we've shown in this report, it is not difficult to relate parameter error to boresight and focus error. The wave theory lends itself readily to being programmed for computer. We have made little about the fact that boresight and focus are vectorial; this is implicit in the fact that the errors of one component can be cancelled by those of another. We have also said little about statistics, which do apply in the limit. The answer to the random walk problem is the same for vectors as it is for scalers, if the number of variables is great enough.

We've assembled a great deal of general material that should be of use in preliminary layout, but we warn that much of the data is of questionable accuracy. Some of the materials are exceedingly nonlinear, particularly plastics and fluids. The data supplied is intended for use only in the initial stage of design, with the manufacturers to be consulted prior to optimization.

The design of athermal systems depends on selecting the right materials and upon employing a good design technique. We are inclined to think design technique is more important than material selection, but this is merely a matter of opinion. We have offered some ideas on the design of athermal systems. We're sure the reader will see opportunities of his own.

6.2 RECOMMENDATIONS

We recommend further investigation of the effects of thermal gradients. We believe emphasis can now be directed toward practical optics rather than the simple abstractions dealt with in the present report. We would like to recommend a collaboration between Dr. Buchroeder, author of this report, and Dr. Malvick, professor of engineering on joint appointment with the Optical Sciences Center of the University of Arizona. Dr. Malvick is well versed in the finite element computer analysis of optical elements, and well qualified to quantify the effects of convection, conduction and radiation.

We recommend a parallel experimental investigation of mock instruments built to yield data on the success or failure of mathematical modelling. Since the image forming qualities of such instruments are

not directly important, they may be of uniquely economical design.

Following the completion of theoretical and experimental research, we recommend that an unclassified military optical system, such as an aircraft periscope, be analyzed and tested in the framework of theory.

SELECTED BIBLIOGRAPHY

Acitelli, M. A. et al, "Light Weight Optical Materials", AFAL-TS-65-182 (1966)

Alvarez, L. W., USP 3,378,326 (1968), "Gyroscopically controlled accidental motion compensator for optical instruments"

Alvarez, L. W., USP 3,434,771 (1969), "Gyroscopic Lens"

American Institute of Physics Handbook, 3rd Ed., McGraw-Hill, New York (1957)

Berggren, R. R., and G. E. Lenertz, "Feasibility of a 30-Meter Space Based Laser Transmitter", NASA CR-13903 Final Report (1975)

Branigan, A. E. O., USP 3,424,523 (1969) "Gyroscopically stabilized lens"

Briers, J. D., "Interferometric Testing of Optical Systems and Components: a Review", Optics and Laser Technology, Feb. 1972, p. 28.

Buchroeder, R. A., "Thermal Compensation of Focus", internal correspondence, Hughes Aircraft Company (1973)

Buchroeder, R. A., Tilted Component Optical Systems, PhD dissertation, University of Arizona 1976

Call, D. D., USP 3,424,522 (1969), "Stabilized optical system"

CODE 5 Designer's Manual, Optical Research Associates, Pasadena, CA. (1975 + updates through 8/78).

Corning Glass Co., Low expansion materials booklet

Drodofsky, M., USP 3,377,910 (1968), "Stabilized Optical Instrument Using Box Level Bubble as Lens"

Engis Equipment Co., "Penta Prism Behavior in Optical Tooling Techniques", Chicago, Ill. (no date, ca. 1960)

General Electric Co., Fused quartz catalog

Grey, David S., "Tolerance Sensitivity and Optimization", Applied Optics, 9, 3, 523 (1970)

Grey, D. S., USP 2,453,218 (1948) "Image forming Optical Lens System Athermalized for Focal Point"

Gross, R. A. "Analysis of Internal-Inertial Image Stabilization", Applied Optics, 10, 6, 1422 (1971)

Handbook of Optics, McGraw-Hill, New York (1978)

Harper, K. W., USP 3,389,950 (1968) "Fiber Optics Scan System"

Heflinger, L. O., et al, USP 3,504,957 (1970) "Optical Stabilized Telescope Arrangement"

Heflinger, L. O., USP 3,460,881 (1969), "Image Stabilizer"

Henson, Truman, Binoculars, Telescopes and Telescopic Sights Greenberg, New York (1955)

Hopkins, H. H. "The Aberration Permissable in Optical Systems", Proc. Phys. Soc., 70, 5B, 449 (1957)

Hopkins, H. H., "The Frequency Reponse of Defocused Optical Systems", Proc. Roy. Soc. A. 231, 91 (1955)

Hopkins, H. H., Wave Theory of Aberrations, Clarendon Press, Oxford (1950) (now available from University Microfilms)

Hopkins, H. H., and H. J. Tiziani, "A Theoretical and Experimental Study of Lens Centering Errors and their Influence on Optical Image Quality", Brit. J. Appl. Physics, 17,33 (1966)

Jamieson, Thomas H., "Thin-lens Theory of Zoom Systems", Optica Acta, 17, 8, 565 (1970)

Johnson, B. K., Optics and Optical Instruments, Dover, New York (1960)

King, W. B., "Unobscured Laser-Beam-Expander Pointing System with Tilted Spherical Mirrors", Applied Optics 13,1,21 (1974)

Kingslake, Rudolph, Lens Design Fundamentals, Academic Press, NY (1978)

Kohler, H., and F. Strahel, "Design of Athermal Lens Systems", in Space Optics, Proc. ICO-9 (1972)

Koppensteiner, A. H., USP 3,424,521 (1969), "Stabilized offset lens"

Krynin, L. I., "Probability analysis of the centering accuracy in commercially manufactured objectives" Soviet Journ. Opt. Tech., 44, 11, 664 (1977)

Levi, L., and R. H. Austig, "Tables of the Modulation Transfer Function of a Defocused Perfect System", Applied Optics, 7,967 (1968)

Levy, Samuel J., Applied Geometric Tolerancing, TAD Products Corp., Beverly, MA. (1974)

Malvick, Allan J., 'thermal analysis of prisms', private communication between R. Light and A. Malvick, (1978)

Martin, L. C., Optical Measuring Instruments, Blackie and Son, Ltd., London (1924)

Materials Selector, Reinhold Pub. Co., Stamford, Conn. (1977)

Moffitt, G. W., "Compensation of Flexure in Range Finders and Sighting Instruments", JOSA, 37, 7, 582 (1947)

Mukojima, Michi, USP 3,414,344 "Flexible Optical System for Transmitting Light or Optical Images".

Myers, Frank, "Thermal Compensation of Optical Systems", internal presentation, Hughes Aircraft Company, (1974)

Optical Coating Laboratories, Inc., Coatings and Filter Properties, loose leaf folder

Owens-Illinois Co., CER-VIT brochure

Perry, J. W., "Thermal Effects upon the Performance of Lens Systems", Proc. Physical Society., 55, 4, 17 (1943)

Reitmayer, F., and H. Schroeder, "Effect of Temperature Gradients on the Wave Aberration in Athermal Optical Glasses", Applied Optics, 14, 3, 716 (1975)

Richey, Charles A., "Aerospace Mounts for Down-to-Earth Optics", Machine Design, Dec. 1974, p. 121.

Rimmer, M., "Analysis of Perturbed Lens Systems", Applied Optics, 9,3,533 (1970

Schott Optical Glass Company, Catalog No. 3050/72 and updates through 8/78

Seyrafi, Khalil, Ed. "Engineering Design Handbook of Infrared Military Systems, Part One", AMCP 706-127 (1971)

Shack, R. V., "The Influence of Image Motion and Shutter Operation on the Photographic Transfer Function", Applied Optics, 3, 10, 1171 (1964)

Shannon, R. R., et al, "Preliminary Design of a Collimator and Target Simulator", prepared for Air Force Weapons Laboratory, Kirtland AFB, by Optical Sciences Center, University of Arizona, (1977)

Smith, Albert E., USP 3,454,330 (1969) "Coherent Optical Joint".

Smith, Warren J., Modern Optical Engineering, McGraw-Hill, NY (1966)

Sokol'skiy, M. N., "Measurement Errors in Instruments Exhibiting Nonsymmetrical Such as Coma and Lateral Color", Sov. Journ. Opt. Technology., 39, 9, 538 (1972)

Steel, W. H., "The Defocused Image of Sinusoidal Gratings", Optica Acta, 3, 2, 65 (1956)

Strang, J. M. et al, USP 3,133,143 (1964), "Periscopes with compensation for Image Motion Caused by Bending".

Tew, Jr., E. James, "Measurement Techniques Used in the Optics Workshop", Applied Optics, 5, 5, 695 (1966)